To the Graduate Council:

I am submitting herewith a thesis written by Thomas W. Allen entitled "An Experimentally Verified Computer Model of a Passive Solar Modular House." I have examined the final copy of this thesis for form and content and recommend that it be accepted in partial fulfillment of the requirements for the degree of Master of Science, with a major in Mechanical Engineering.

Robert Reid, Major Professor

We have read this thesis and recommend its acceptance:

Accepted for the Council:

Vice Chancellor
Graduate Studies and Research

AN EXPERIMENTALLY VERIFIED COMPUTER MODEL OF A PASSIVE SOLAR MODULAR HOUSE

A Thesis

Presented for the

Master of Science

Degree

The University of Tennessee, Knoxville

Thomas W. Allen

August 1981

3053775

ACKNOWLEDGEMENTS

It is doubtful that this work would have been completed without the love, support, and many hours of hard work by the author's fiancee during these past months. Thank you, Nancy.

Additional thanks are extended to Dr. Robert Reid for his many helpful suggestions, Dan Roeder and David Chaffin for their help with computer problems, and Bernie McGraw for his work in preparing the experimental portion of this study.

Finally, the financial support provided by the Tennessee Valley Authority and the Energy Environment and Resources Center is gratefully acknowledged.

ABSTRACT

The performance of a 111-m^2 passive solar modular house located on The University of Tennessee campus was modeled by a modified version of the computer program TRNSYS. A computer model was written and experimentally verified for the 20 clear water-filled tubes in the house.

The test house was supplied by the Tennessee Valley Authority (TVA) for study to determine the system's performance both experimentally and analytically. The building is a heavily-instrumented version of one of several passive designs that TVA has approved as a part of its incentive program to make passive solar modular homes available to the public. The five-room house is of conventional wood construction, well insulated, and tightly built. The passive heating system consists of 14.66 m^2 of south-facing glass fitted with insulating shades and 20 water-filled tubes. Each tube is 0.305 m in diameter and 2.13 m tall and made from a fiberglass material. Various temperatures throughout the house and weather data at the test site have been collected each hour since April 15, 1981. These items are recorded by a computerized data acquisition system.

The house was simulated using subroutines supplied by TRNSYS representing components of the system. Experimental work was used to verify parts of the model not supplied with TRNSYS. A subroutine used to convert solar radiation measured at 45 degrees, as was done at the test site, to horizontal radiation as required by the computer program was verified from experimental information supplied by TVA. The portion of the tube model used to determine the amount of solar radiation

transmitted by the water was independently verified at the test site by a system of pryanometers. Finally, the tube model itself was verified by comparing predicted and measured temperatures of the water in the tubes for a period of 504 hours. This verification showed the tube model predictions to be within three percent of the measured data.

Using heating season data from a typical year, the performance of the system and several alternatives was simulated. The house, as designed, required ten percent less auxiliary energy than the same house without water tubes, and 46 percent less energy than the same house with conventional amounts of south glass and no tubes or night insulation. An examination of the need for window insulation, used during the night, showed that the shades reduced the need for auxiliary heat by 24 percent.

TABLE OF CONTENTS

CHAPTER		PAGE
I.	INTRODUCTION	1
	Passive Solar Energy Systems	1
	Passive Solar and Modular Homes	5
	The TVA-UT Passive Solar Modular House	5
	Computer Modeling	10
II.	COMPONENT MODELS	12
	Transfer Function Method of Modeling Heat Flows	13
	Attic Model	14
	Wing Wall and Overhang Model	15
	Window Model	17
	Cylindrical Tube Model	20
	Heating Load Calculation	29
	Solar Radiation Models	34
	Component Configuration	38
III.	EXPERIMENTAL VALIDATION	41
	Determination of Extinction Coefficient for Water	42
	Validation of the Radiation Convertor	45
	Validation of the Kalwall Tube Model	45
IV.	HEATING SEASON SIMULATION RESULTS	51
	Heating Season Weather Data	51
	Alternative Systems Performance	52
	The Impact of Night Insulation	52
	The Impact of Storage	54
	An Evaluation of the MRT	56
V.	CONCLUSIONS	58
	The Passive Modular House Computer Work	58
	The Passive Modular House Design	59
LIST OF REFERENCES		61
APPENDICES		66
Appendix A		67
Appendix B		69
Appendix C		72
Appendix D		73
Appendix E		91
VITA		94

LIST OF TABLES

TABLE		PAGE
1.	Comparison of Passive Solar Alternatives for a Heating System	53
2.	Temperature of Surfaces Used to Calculate the MRT in the Passive House from 6:00 p.m. to 12:00 Midnight on January 3rd	57

LIST OF FIGURES

FIGURE		PAGE
1.	A direct gain system	2
2.	Mass wall	3
3.	Sunspace	4
4.	Location of Kalwall tubes in the passive house	7
5.	A vertical section through the modular house showing the bay window and a water tube	8
6.	Total and spectral transmittance of Kalwall	9
7.	Overhang and wing wall shading a receiver	16
8.	Location of passive modular house between ACES house and control house	17
9.	Example of shading of beam radiation by adjacent tubes	22
10.	Approach used to determine average path length traveled in the tube	24
11.	Radiation exchange between a tube and its surroundings	26
12.	The influence of infiltration rates on building heating requirements	33
13.	Beam and diffuse radiation striking a tilted surface	35
14.	Radiation convertor logic	37
15.	TRNSYS component configuration	40
16.	Equipment layout for the experimental determination of the amount of sunlight trapped by the water in a Kalwall tube	44
17.	Comparison of calculated and measured radiation on a horizontal surface for the day of March 31, 1981	46
18.	TRNSYS component configuration for tube model verification	49

FIGURE PAGE

19. Measured and calculated tube temperatures for April 22, 1981 50

20. Room temperature with and without tubes 55

21. South wall of living room in passive modular house 92

LIST OF SYMBOLS

Symbol	Description	Units
A	area	meters^2
A_{TN}	tube north surface	
A_{TS}	tube south surface	
A_g	glazing	
AA	empirical constant for infiltration rate	air changes/hour
BB	empirical constant	air changes/hour • °F
b_n	time-dependent temperature-related transfer function at time n	kilojoules/meters^2 • hours • °C
C	empirical constant for free convection	
C_p	constant pressure specific heat	kilojoules/kilogram • °C
DD	empirical constant for infiltration rate	
d_n	time-dependent heat flux-related transfer function	
E	black body emissive power	kilojoules/meters^2
E_{b1}	body one	
E_{b2}	body two	
F	shape factor	
F_{1-2}	area one to area two	
F_{p-1}	person to area one	
F_{p-n}	person to nth area	
Gr_f	Grashof number evaluated at film temperature	
H	total radiation on the horizontal	kilojoules/meters^2 • hour

Symbol	Description	Units
H_b	beam radiation on the horizontal	kilojoules/meters^2 · hour
H_d	diffuse radiation on the horizontal	kilojoules/meters^2 · hour
H_D	extraterrestrial radiation on the horizontal	kilojoules/meters^2 · hour
H_T	total radiation on a tilted surface	kilojoules/meters^2 · hour
h_{ci}	convection heat transfer coefficient inside surface of glazing	kilojoules/meters^2 · hour · °C
h_r	radiation heat transfer coefficient	kilojoules/meters^2 · hour · °K
h_{TN}	north side of tube	
h_{TS}	south side of tube	
In	infiltration rate	air changes/hour
I(L)	radiation intensity at some depth of water (L)	kilojoules/meters^2
I(0)	radiation intensity at the surface	kilojoules/meters^2
J	radiosity	kilojoules/meters^2
K	extinction coefficient	meters^{-1}
K_f	thermal conductivity at the film temperature	kilojoules/meters^2 hour · °C
KT	ratio of horizontal to extraterrestrial solar radiation	
L	depth or length	meters
M	mass	kilograms
nd	number of days	days
$\overline{Nu}$	average Nusselt number	
Pr_f	Prandlt number at film temperature	

Symbol	Description	Units
Q	heat transfer rate	kilojoules/hour
Q_{thru}	through the water in one tube	
Q_{solar}	of solar energy entering one tube	
q	heat transfer rate	kilojoules/meters^2 . hour
q_o	at present time	
q_n	at time n	
q_{1-2}	between areas one and two	
R	ratio of H_T to H	
R_b	shape factor between tilted receiver and solar beam radiation	
S	tilt angle of receiver	degrees
Sc	solar constant	kilojoules/meters^2 . hour
T	temperature	°C
T_a	ambient	
T_{CR}	crawlspace	
T_{gi}	glazing inside	
T_G	ground	
T_r	room	
$T_{sa,n}$	solair at time n	
t	time	
$\dot{T}$	absolute temperature	°K
$\dot{T}_a$	ambient	
$\dot{T}_{CL}$	clothing	
$\dot{T}_g$	glazing	
V_w	velocity of wind	miles/hour

Symbol	Description	Units
β	percentage of solar radiation absorbed by water in first few centimeters	
ε	emittance	
ε_g	glazing	
ε_1	area one	
ε_2	area two	
ρ	reflectance	
$\rho_{\parallel}$	parallel component	
$\rho_{\perp}$	perpendicular component	
τ	transmittance	
θ_H	angle of incidence with horizontal	degrees

CHAPTER I

INTRODUCTION

Passive Solar Energy Systems

Solar heating can be described as the collection, storage, and delivery of solar energy to a living space. Passive solar energy is distinguished from other types of solar heating systems by the manner in which this energy transfer occurs. In passive designs, transfer of solar energy from collector to storage and subsequent delivery from storage to living space is done without the aid of mechanical devices (e.g., fans or pumps). The U.S. Department of Energy (DOE) defines any system that uses mechanical devices to aid heat transfer in only one of these two loops as a hybrid system, while a system with mechanical aid in both loops is termed an active solar heating system.[1]

Fifty percent of the body's heat loss is by radiation. Because of this, an effective way to warm individuals in a room is to raise the temperatures of large areas of the walls or floor in that room above body temperature. Since this is done in many passive heating systems, passive solar heating can be more efficient than convective systems which heat room air.[2] A measure of the effectiveness of a radiant heating system is the mean radiant temperature (MRT). The MRT is defined by Fanger as ". . . that uniform temperature of black surroundings which will give the same radiant heat loss from the person as the actual case under study."[3] There are several formulas relating dry bulb temperature and MRT. One of the most widely accepted is an empirical equation

developed by Raber and Hutchinson.[4] This equation states that the dry bulb temperature in a room required to maintain a sensation of 21°C with a given MRT can be calculated by: T_{room} = 42.2°C - MRT. Hence, a measured MRT of 25°C would require a room dry bulb temperature of only 17.2°C to give the 21°C sensation.

The major passive systems are: direct gain, thermal storage wall, and attached sunspace. As shown in Figure 1, the direct gain approach

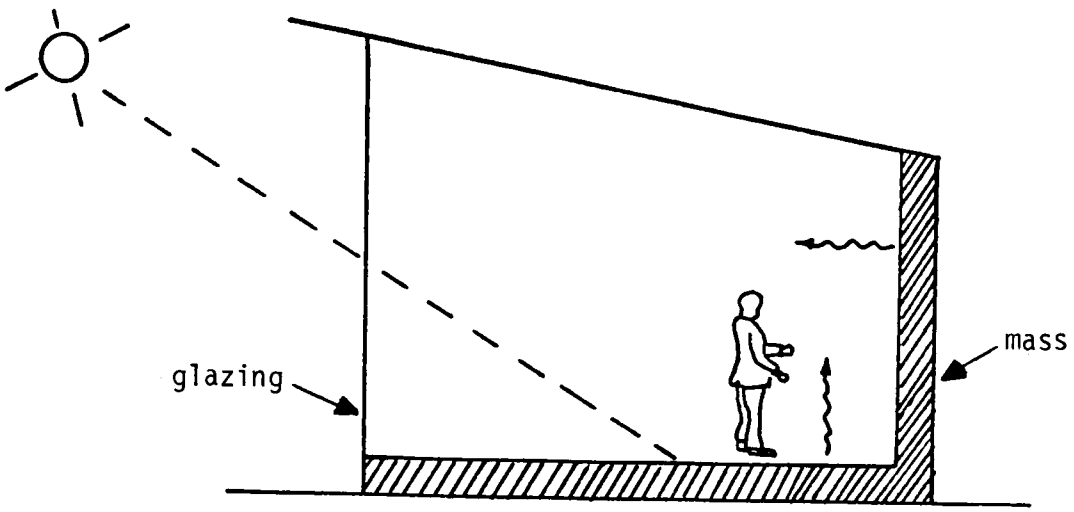


Figure 1. A direct gain system

calls for sunlight to pass through the living space before it strikes the storage mass. This sunlight may enter the room through vertical glass, skylights, or clerestories. Items with low thermal storage capacity in the direct gain room will cool off quickly when not in

direct sunlight. The storage mass will then radiate energy to any item in the room with a lower surface temperature than itself.

The thermal storage wall shown in Figure 2 is a large mass which is placed only 0.05-0.12 m from south-facing vertical glass. The outer

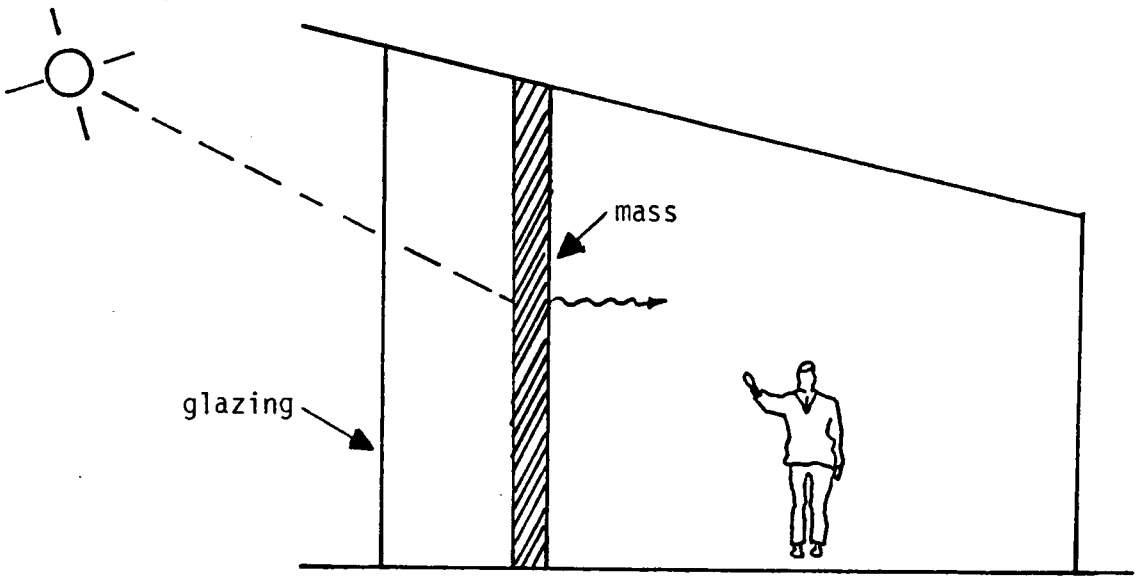


Figure 2. Mass wall

surface of this wall receives solar energy which slowly conducts through the wall and radiates into the living space. Because of the time needed for the energy to move to the room side of the wall, energy falling on the wall is not transmitted to the living space until several hours after it strikes the wall's outer surface.

Attached sunspaces are usually greenhouses or atriums, as shown in Figure 3. Temperatures in these areas are allowed to rise above

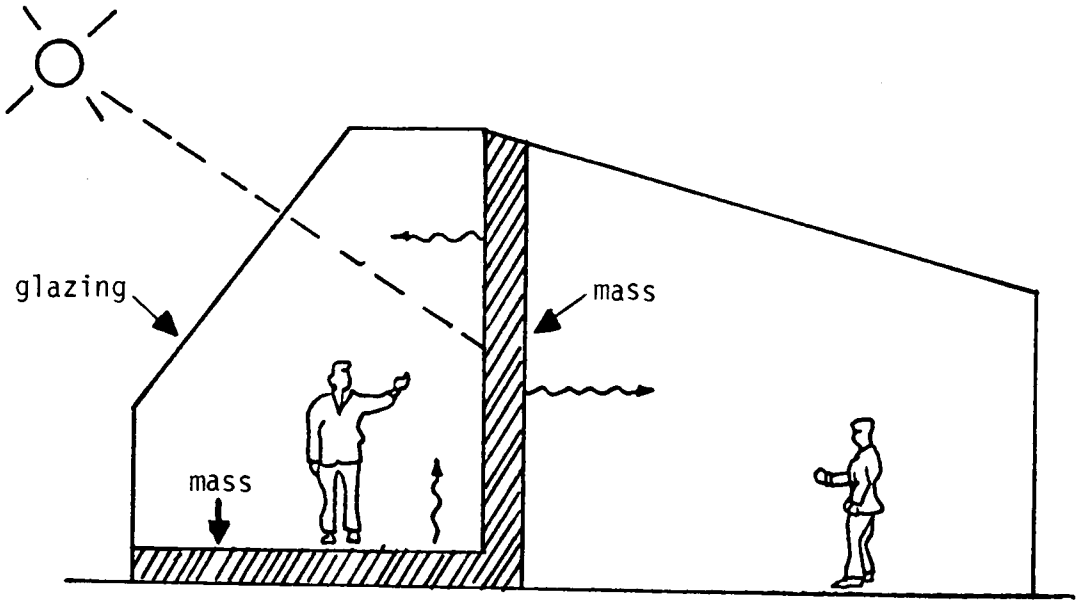


Figure 3. Sunspace

normal levels of comfort for living spaces in order to collect and store as much energy as possible during daylight hours. This energy is usually transferred through a wall common to the sunspace and living space by conduction. This wall performs in a manner similar to the thermal storage wall.

Control of the energy flows in a passive system is provided by overhangs, window insulation, and properly sized storage. The storage material retains energy for later transfer to the living space and absorbs excess energy during periods of intense sunlight, thereby preventing overheating.

The most commonly used storage material for site-built homes is masonry. Water, with its high heat storage capacity, is the next most popular storage medium. Phase-change materials, such as eutectic salts, are used to a lesser extent.

Passive Solar and Modular Homes

Modular homes are built in factories using assembly-line techniques. Most of these homes are constructed from conventional building materials. Transportation considerations usually necessitate the building of the structure in two or more pieces. The separate parts, finished in the factory, are then joined on the foundation.

Several public and private organizations have introduced passive solar heating systems into modular homes.[5] These homes utilize all three major passive solar schemes. Thermal storage is usually provided by water, and attached sunspaces are generally site erected greenhouses.

The major advantage of modular homes is the cost. The average modular home, including foundation and all hook-ups, costs about $\$270/m^2$.[6] A comparable site-built home would cost from $\$322\text{-}377/m^2$.[7]

The Tennessee Valley Authority (TVA) has developed the use of passive solar heating in low-cost modular homes by working with area modular home builders.[8] Passive modular homes built by area manufacturers have been installed throughout the TVA service district.

The TVA-UT Passive Solar Modular House

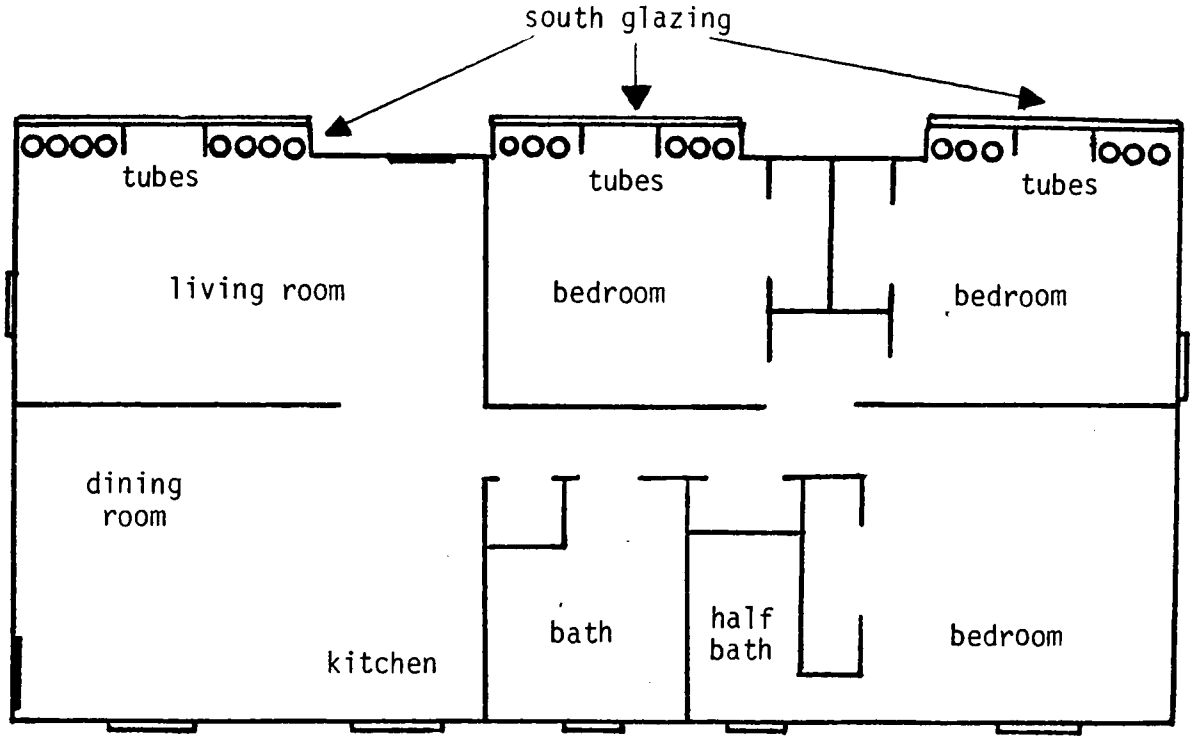
In an effort to evaluate the performance of one of its approved designs under controlled conditions (no one living in the house), TVA has purchased a modular house and installed it at the Tennessee Energy

Conservation in Housing (TECH) site operated by The University of Tennessee, Knoxville (UT). The house is a heavily instrumented version of the Bayside line manufactured by Dixie Royal Homes of Cookeville, Tennessee. The 111-m^2 house has an insulating value of 0.93 m^2 • °C • hr/kJ in the walls, 1.85 m^2 • °C • hr/kJ in the ceiling, and 0.93 m^2 • °C • hr/kJ in the floor.

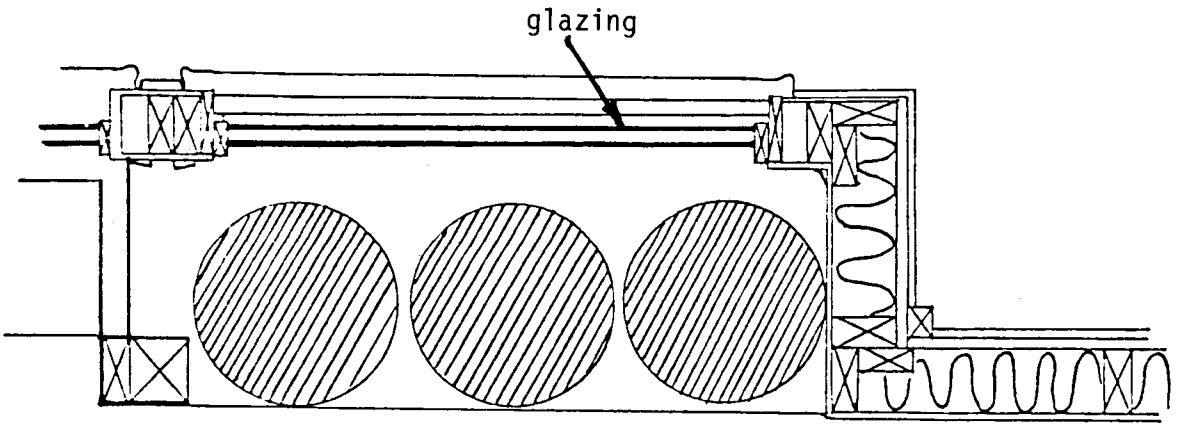
The passive solar heating system consists of 14.66 m^2 of south-facing thermopane glass and 20 translucent water-filled tubes. Figure 4 shows the location of the 20 tubes in the passive house, while Figure 5 is a vertical section through the south glass and tube area. The fiberglass tubes are distributed along the south side of the structure, with eight in the living room and six in each of the two south-facing bedrooms. Each tube is 0.305 m in diameter and 2.13 m tall, giving it a capacity of 155.6 L.

Since the water-filled tubes were placed a few centimeters behind the south glass, the passive system in the modular house is a mass wall design. This mass wall is somewhat unique, however, in that the tubes allow some of the incoming sunlight to pass through. The south-facing rooms are thus filled with a pleasant diffuse light.

The water tubes were manufactured by the Kalwall Corporation of Manchester, New Hampshire. The fiberglass used in their construction had solar transmission characteristics very similar to glass.[9] Figure 6 shows the transmission of solar energy by glass and the Kalwall fiberglass. Work done by the Kalwall Corporation indicates that 50 to 55 percent of the sunlight striking a tube is transmitted through it.[10]



A. Plan view of the passive house showing tube locations



B. Detail of tube location in one window

Figure 4. Location of Kalwall tubes in the passive house

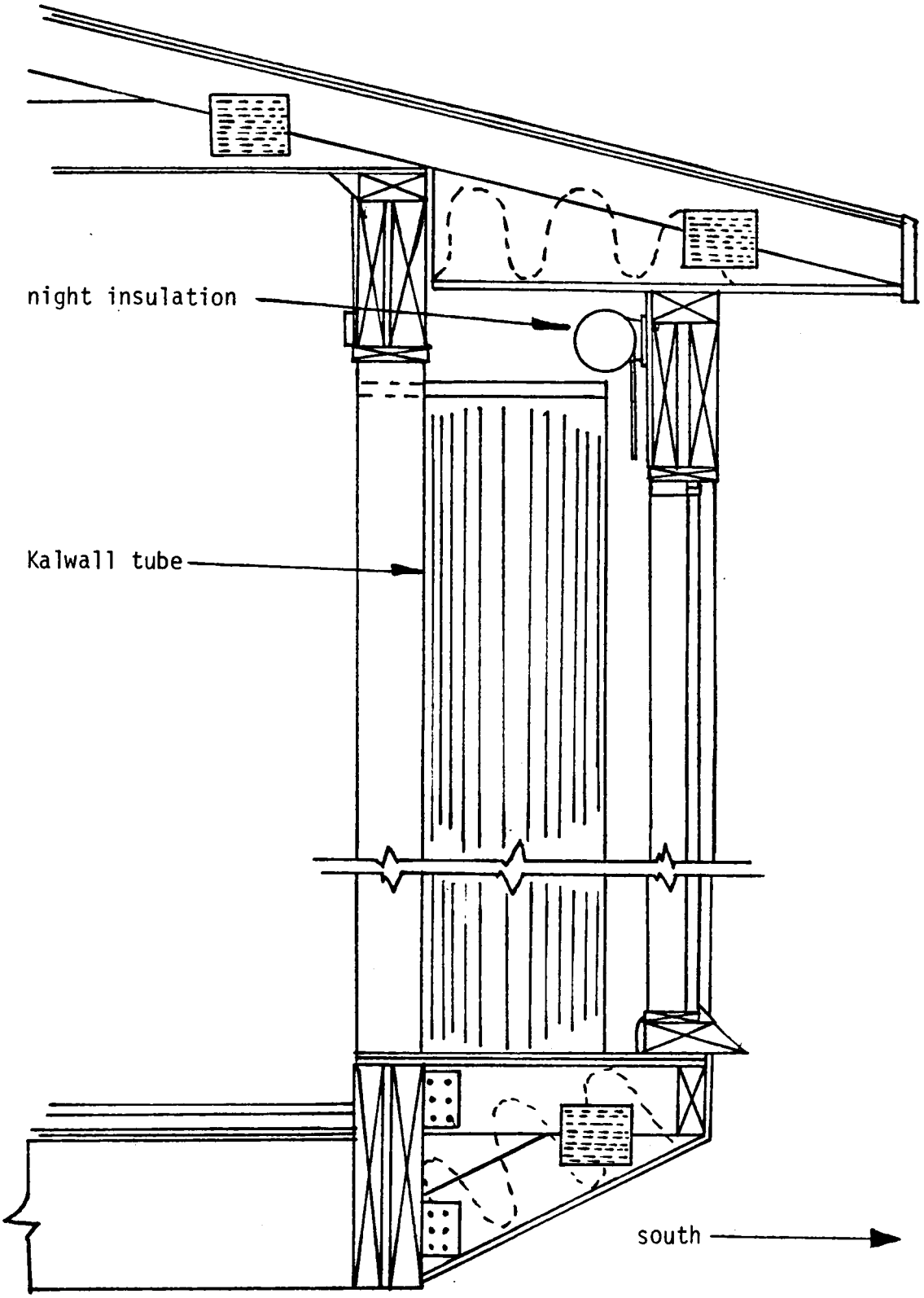
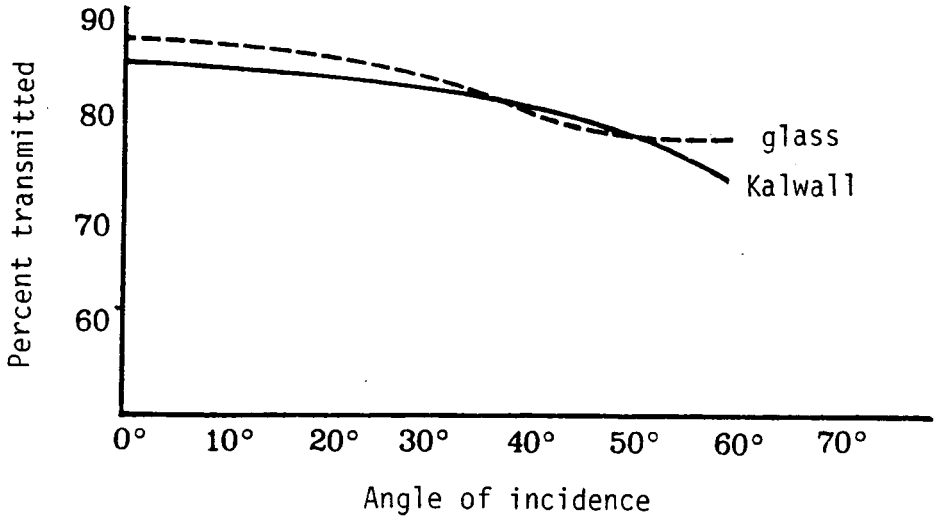


Figure 5. A vertical section through the modular house showing the bay window and a water tube



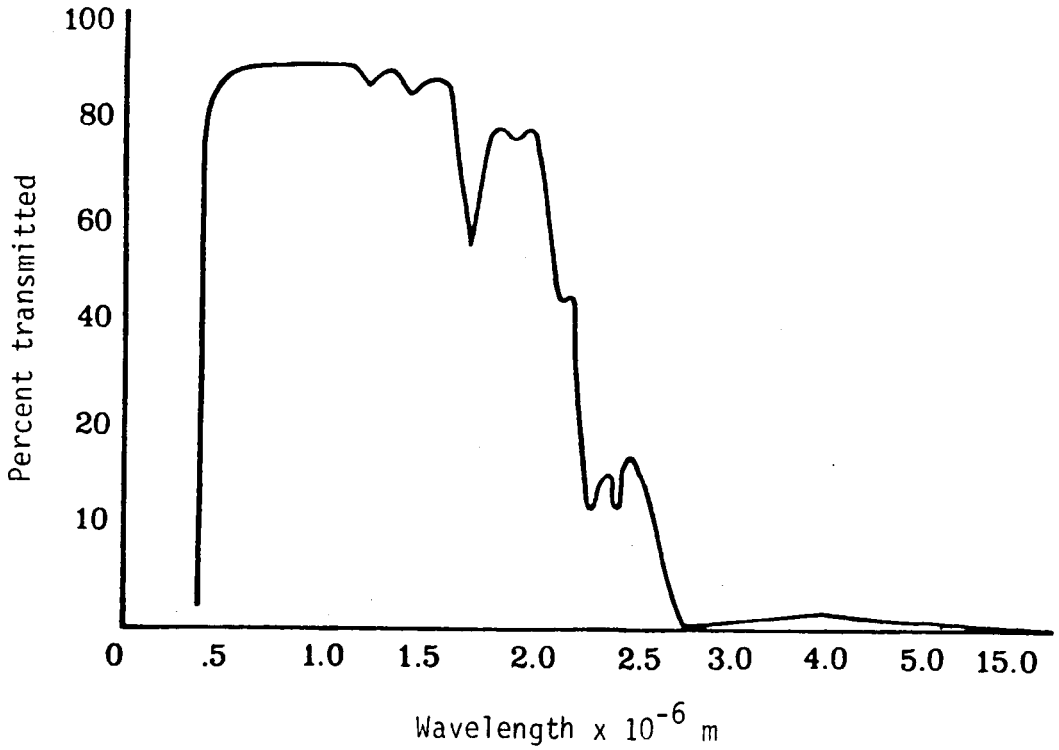


Figure 6. Total and spectral transmittance of Kalwall

In addition to its ability to transmit light, water thermal storage is a good choice for use in a modular home for the following reasons:

1. The water system is less expensive to construct than most other storage systems.
2. Water has a heat storage capacity nearly five times greater than masonry.
3. The mass of the storage system need not be added until the house is installed at the site.
4. Since the water containers are generally not part of the structure, great flexibility is provided in moving storage or changing the amount of storage.

Night heat loss from the tubes is reduced by insulating curtains. Studies have shown that heavy night insulation can cut waterwall heat loss to the outside by more than 50 percent.[11] The night insulation used in the passive modular house was manufactured by the Appropriate Technology Corporation of Brattleboro, Vermont. The window quilt has an insulating value of 0.137 $m^2 \cdot °C \cdot hr/kJ$.[12]

Computer Modeling

Many graphical and simplified computer models are available for analysis of passive systems; however, these models cannot predict room temperature on an hourly basis using actual weather data.[13,14,15,16] Several more complex models are available.[17] A survey was made of these larger programs to determine which one would be best suited for this study. The computer program TRNSYS, developed by the University of Wisconsin, was selected for the simulation work developed in this

document because of its flexibility, ease of use, availability, and adaptability to the university's computer system.[18]

The program reads weather data on an hourly basis. The various building components are simulated by separate subroutines available in the program, thereby allowing for excellent model flexibility. The development and function of major component models used in the building simulation are discussed in the next chapter.

CHAPTER II

COMPONENT MODELS

Since passive systems are usually an integral part of the building, modeling the heating system performance mainly consists of simulating energy flows and temperature responses of the structure itself.

The latest version of TRNSYS, 10.1, contains separate subroutines which model windows, walls, attics, shading devices, and various heating and cooling systems. In addition, several auxiliary subroutines, such as data readers, radiation processors, and printers are available.[18] The TRNSYS computer program includes every subroutine needed to model the passive modular house except a water tube and a crawl space model. A program was written to model the water tubes, and modifications were made in the window and room temperature models to make them compatible with the water tube simulation. Additions were made to the room model to simulate the heat loss through the house floor above a crawl space. Model accuracy and flexibility were improved by adding the options of variable convection coefficients on the exterior of the south glass and infiltration rates into the room model.

Two auxiliary subroutines were also written. The first prints the room temperature and weather conditions each time the room temperature rises above a specified level. The second program calculates direct and diffuse radiation on a horizontal surface from a measured value of total radiation at any angle or orientation.

Transfer Function Method of Modeling Heat Flows

With limited means to control energy collection and distribution, and only short-term energy storage, the room temperature in a passively heated house is a strong function of the weather conditions.

TRNSYS offered two methods of modeling the structure; one was a simple steady-state UA factor method, and the other used transfer functions.[18] The transfer function method of energy flows was chosen because of its ability to accurately simulate hourly responses of the building skin and room temperature to changing weather conditions. While steady-state UA methods may provide accurate energy usage information over long periods of time, they do not provide an adequate response to hourly weather data.[19] These hourly responses are extremely important in predicting thermal comfort in a passively heated house.

The transfer function method and its predecessor, the thermal response factor method, have been used by ASHRAE for over 15 years to calculate cooling loads.[20,21] Several well known and experimentally verified computer programs, such as DOE-2 and NBSLD, are now employing the transfer function method to calculate both heating and cooling loads for buildings.[22,23]

Simply speaking, transfer functions are a time series response to a particular excitation.[24] TRNSYS uses transfer functions in its wall conduction model, attic model, and room model. Transfer functions were used in the room model by specifying the building construction as light, medium, or heavy. A set of functions developed by ASHRAE for each weight of construction was used to account for the time lag between the input of solar radiation and the temperature rise of the room.[20] This lag

occurred because radiation heats up the walls and furnishings of a room, and they, in turn, heat the room air.

The development of the transfer function wall models in TRNSYS followed the original work of Stephenson and Mitalas.[25] Stephenson and Mitalas solved the classical heat conduction equation through a homogeneous substance by the use of Laplace transforms. This solution led to Equation (1) as expressed by ASHRAE:[20]

$$q_o = \sum_{n=0} b_n(T_{sa,n} - T_r) - \sum_{n=1} d_n q_n \qquad (1)$$

The b_n transfer functions are the time response of a particular wall type to a unit change in the inside and outside temperatures. The d_n transfer functions are the wall's time response to a unit pulse of heat flux. The summation is carried out until the b_n and d_n coefficients are of negligible size.

The b and d coefficients used in this program were calculated by a computer program developed by Mitilas and Arseneault.[26] A sample input and output for the exterior wall of the passive modular house is shown in Appendix A.

Attic Model

The attic model provided by TRNSYS calculated an effective sol-air temperature as a function of the sol-air temperature of the various roof surfaces and the infiltration rate. ASHRAE defines the sol-air temperature as the temperature of the outdoor air that, in the absence of all radiation exchanges, would give a rate of heat transfer equal to that which actually takes place in the presence of these radiation exchanges.[20]

The effective sol-air temperature was then used to calculate the heat flux through the floor of the attic. The equation for this heat transfer was the same as the one used in the wall model described in the previous section.

The biggest challenge facing the user of this subroutine was calculating the attic ventilation rate. ASHRAE provided empirical equations for natural ventilation as a function of wind velocity, temperature difference, and area of the openings. These equations were applied to provide an estimate of the number of air changes per hour the attic would have under typical winter conditions. The value was found to be approximately one. The ventilation rate was varied from one to four air changes per hour to check the effect of the rate on the amount of heat transferred through the ceiling. This variation increased the heat transferred through the ceiling by only 0.41 percent. This slight change showed that under winter conditions, the amount of heat transferred through the ceiling was not a strong function of the attic infiltration rate.

Wing Wall and Overhang Model

The wing wall and overhang model used in TRNSYS calculated the shading produced by these devices on a vertical receiver. Figure 7 shows a typical shading situation produced by the two devices.

The fraction of beam radiation hitting the receiver was calculated by TRNSYS using an ASHRAE algorithm.[20] The shape factors between the receiver and the ground, and the receiver and the sky, were calculated by numerically integrating the differential receiver area radiation view factor of the wing wall or overhang over the receiver area. Calculation

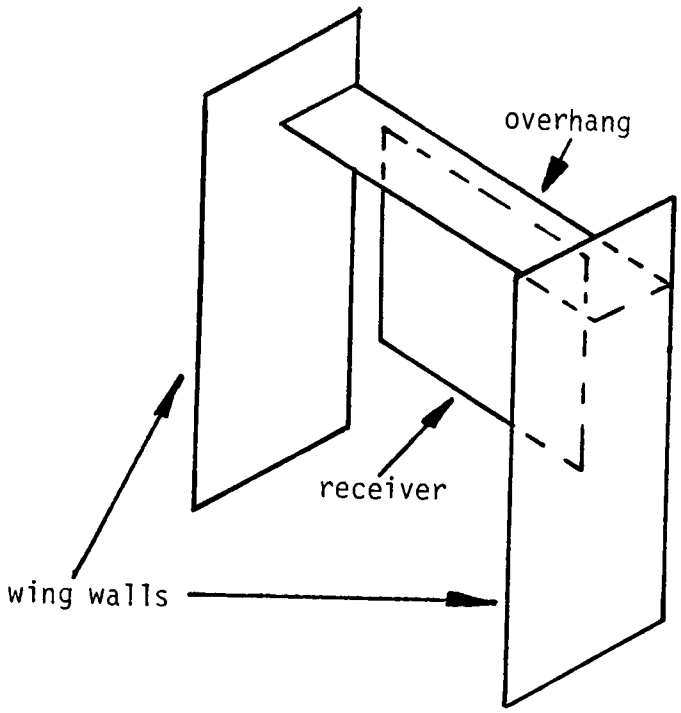


Figure 7. Overhang and wing wall shading a receiver

of these three fractions accounted for the amount of beam, diffuse, and ground reflected radiation striking the receiver. The model assumed isotropic conditions for diffuse and reflected radiation. In addition, it did not account for the radiation reflected off of the shading devices and striking the glazing. The model output was the amount of beam and diffuse radiation per unit area hitting the glass.

An overhang model was specified to account for the shading by the eave of the passive modular house. Three wing wall models were specified to simulate the shading on the three groups of south-facing windows by adjacent buildings. The building layout shown in Figure 8 shows that the passive modular house was placed between and set back 7.12 m from two

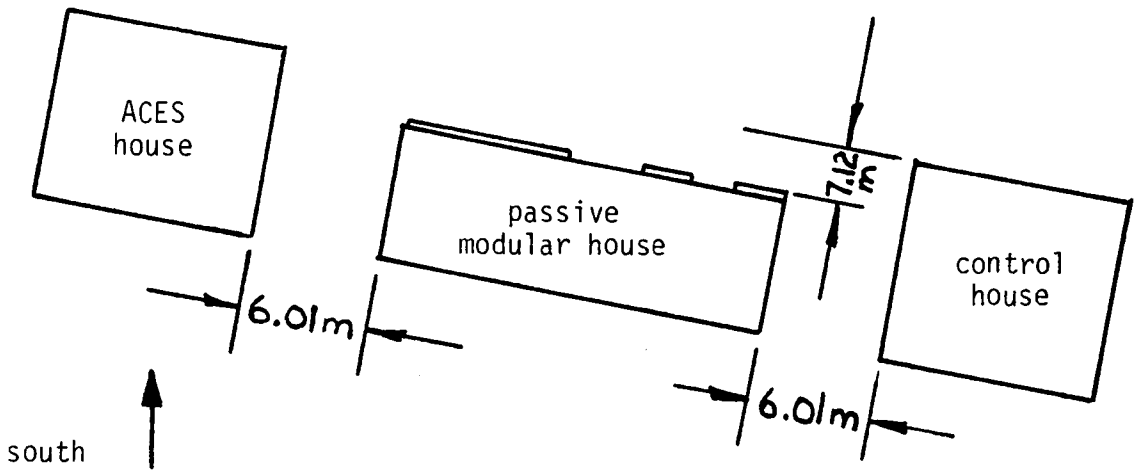


Figure 8. Location of passive modular house between ACES house and control house

buildings. Because the two adjacent buildings had sloping roofs, an average height was used to model them. Computer simulations, run over the heating season, showed that the setback caused only a three percent loss of energy striking the glass.

Window Model

TRNSYS provided a detailed window model. This model calculated the amount of energy a window transmits by radiation and conduction each hour. The transmittance of the glass was calculated each hour as a function of the sun's angle of incidence with the glass.

Fresnels equations were employed in this process. The model assumed that the transmittance of diffuse radiation (including ground reflected radiation) was equal to the transmittance of beam radiation of an angle of incidence of 60 degrees.

In calculating the conduction losses through the window, TRNSYS called for constant values of the inside and outside convection-radiation coefficients. While inside conditions may remain nearly constant, outside window conditions, such as ambient temperature and wind velocity, can vary widely. The contribution of the outside convection-radiation coefficient to the U value of an insulated wall is small. Its significance in the total energy balance increases, however, when a large portion of the exterior surface is a good conductor of heat, such as glass.

In the case of the passive house, the UA product of the south glass is 35 percent greater than the UA product of the remaining walls. For these reasons, the window model was altered to calculate a weather-dependent U value each hour. The expression used for the radiation coefficient is given below:

$$h_r = \varepsilon_g \cdot \sigma \cdot (\dot{T}_g^2 + \dot{T}_o^2) \cdot (\dot{T}_g + \dot{T}_o) \qquad (2)$$

Equation (2) was used by ASHRAE in its development of the sol-air concept.[20] The equation is a portion of the energy balance on a sunlit vertical wall. Under conditions of high solar radiation, the surroundings are at a higher temperature than the ambient air. This compensates for the sky temperature being lower than the ambient air temperature, such that when the shape factors for a vertical surface are included, the effective sky-surroundings temperature is nearly equal to the ambient temperature. Thus, T_a can be used for the effective temperature for the radiation exchange in Equation (2). The temperature of the ambient air was supplied from a weather tape, while the glazing temperature was used

from the previous hour. The glazing temperature was calculated by first solving the UA equation for the glazing, or glazing and night insulation depending upon whether or not the shades were in use. This Q conducted was then applied to the energy balance at the inside surface of the window or insulation, as shown below:

$$T_{gi} = (Q/A_g \cdot h_{ci}) + T_r \qquad (3)$$

The assumptions were made in the development of Equation (3) that the amount of solar energy absorbed by the glass was negligible, and that the temperature of the glass was not appreciably increased by radiation from the tubes.

The solution to the outside convection coefficient h_{co} was developed in two ways. The much-used empirical correlation by McAdams and a more recent empirical relationship by Kimura were added to the model.[27,28] The programmer has the option of choosing one of these. Research into the McAdams relationship showed that the correlation was actually published first by Jurges in a German work in 1924. Kimura's correlation was based upon work done by the Japanese in the early 1970's. While independent experimental verification of these two works was not located, it should be noted that Kimura's correlation accounted for wind direction, while McAdam's did not. A 31-week long computer simulation comparing the two variable coefficients and a constant U value from ASHRAE showed that McAdams's relationship produced 1.3 percent more heat loss through the south glass than Kimura's, while the average loss of the variable techniques was 7.14 percent less than the constant U value model. The computer code for the variable correlations is given in Appendix B.

Conduction losses by this model were calculated with the night insulation up or down. The raising and lowering of the shade was set on a timer. This timer was prevented from lowering the shades when appreciable daylight was left. The conduction losses were fed into the load model, while the radiation input was sent to the tube model described in the following section.

Cylindrical Water Tube Model

Several passive solar programs, including Los Alamos Scientific Laboratory's PASOLE, are able to simulate a water wall in an extremely simplified manner.[29] In PASOLE, the water wall was assumed to be a fraction of the south glass depending upon its projected area. This assumption failed in the case of cylindrical water walls because the angle of incidence varies around the circumference. Hence, the cylinders reflect some energy into the room which was not accounted for by the program. This caused actual room temperatures to be higher than predicted values.[30]

Colorado State University has developed computer models of cylindrical tubes with all or part of the tube surface painted black.[30] These models assume a constant, effective absorptance for the tube. Computer models simulating clear water-filled tubes which predict the amount of energy through the tube are not available.

The cylindrical tube program developed for this study models the energy flows into and out of a single clear tube with tubes on either side of it. This complete computer code for the model appears in Appendix C. The major assumptions used in formulating this energy balance were:

1. Each tube could be modeled as a single node because thermal stratification effects were negligible in the overall energy balance.
2. A tube could be shaded by the tubes to the left and right of it.
3. Radiation passing through or reflecting off of a tube was absorbed by the room and had negligible effects on the energy balance of the adjacent tube.
4. Convection losses off of the top and conduction losses off of the bottom of the tube could be neglected.
5. The radiation exchange between the tube and its surroundings could be satisfactorily modeled as two-dimensional in the horizontal plane.
6. The air temperature between the tubes and glass was equal to the room temperature.

The water wall model, constructed to interact with TRNSYS subroutines, received solar input from the radiation processor after it was passed through the overhang and wing wall model. The tube model was also connected to the room temperature model to determine energy flows between the tube and the room.

The tube subroutine began by calculating the portion of the tubes circumference struck by beam radiation as a function of the location of the sun and the proximity of neighboring tubes. Figure 9 shows a typical early morning situation, with the eastern tube shading the object and the arc struck by beam radiation. This arc was divided into

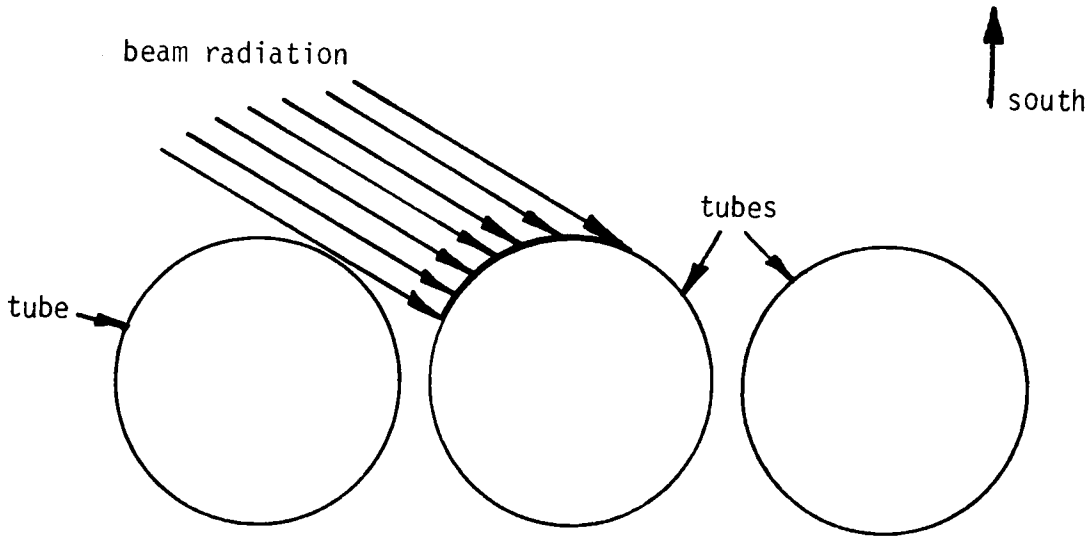


Figure 9. Example of shading of beam radiation by adjacent tubes

one-degree increments. The arc was assumed to be flat across this 0.0027-m-long section. Next, an angle of incidence between the sun's rays and these flat segments was calculated as a function of each segment's azmuth angle.

The transmittance, reflectance, and absorptance of each flat was then calculated using the individual angles of incidence. These properties of the fiberglass were calculated using Fresnel's laws. A constant index of refraction of 1.58 was used.[9] The extinction coefficient was calculated by using a known angle of incidence, a known transmittance, and the given index of refraction. The details of this development are given in Appendix D.

Following the conclusions of Parmalee, the diffuse radiation was assumed to strike the tubes at a mean angle of 60 degrees.[31] Thus, the transmittance reflectance and absorptance of diffuse radiation by the

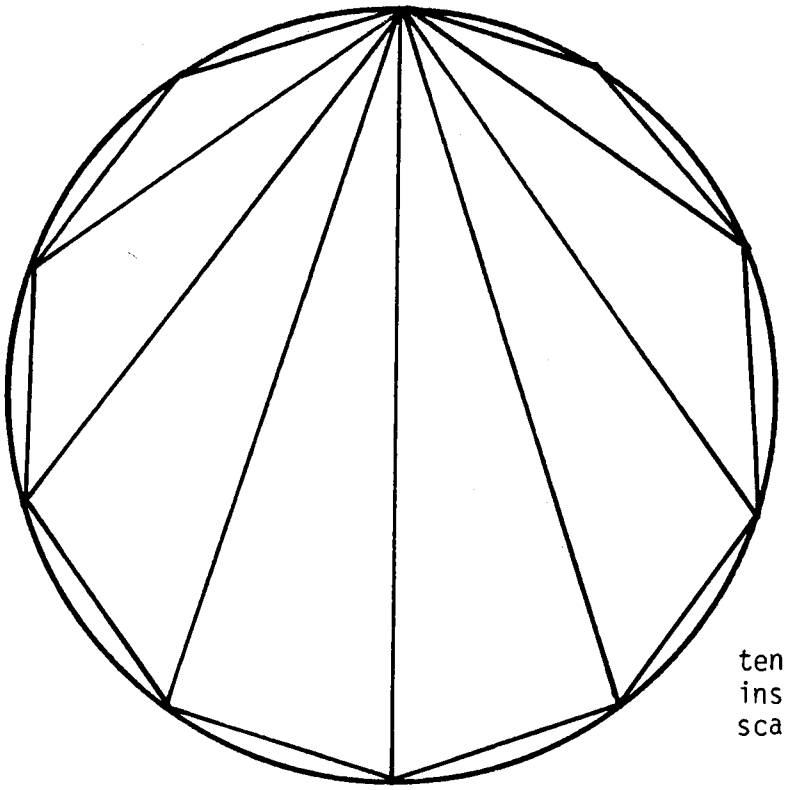
tube were evaluated at that angle. The total amount of beam radiation transmitted, absorbed, and reflected was added to the amount of diffuse radiation in these three categories. The total reflected energy was assumed to be absorbed by the room, while the transmitted portion was attenuated by the water in the tube.

The amount of solar energy transmitted by the water was calculated using an equation developed by Dake and Harleman.[32] The equation is:

$$I(L) = (1 - \beta) \cdot I(0) \cdot e^{-kL} \qquad (4)$$

Equation (4) expresses the amount of radiation reaching a certain depth as an exponential function of the distance traveled, L, minus an initial amount of radiation absorbed at the surface times the radiation intensity at the water's surface. This initial fraction, β, accounted for infrared radiation since solar radiation above 0.9×10^{-6} is absorbed in the first centimeters of travel through water.[9] Dake and Harleman have shown experimentally that β was equal to 0.4 for all of the bodies of water that they tested.[32]

Since the fiberglass tube wall diffuses radiation, an average path length through the water was calculated. This was done by inscribing a 360-sided polygon in a 0.3058-m-diameter circle and numerically calculating an average length of the cords connecting the corners of the polygon. This length was then used as the base of a triangle formed by the sun's rays to calculate a solar path length. This process is shown in Figure 10. Calculating an average path length and then applying it to an exponential equation is justified by the fact that in distances from 0-0.305 m, the relationship between distance traveled and energy



ten-sided polygon inscribed in 1/3-scale tube

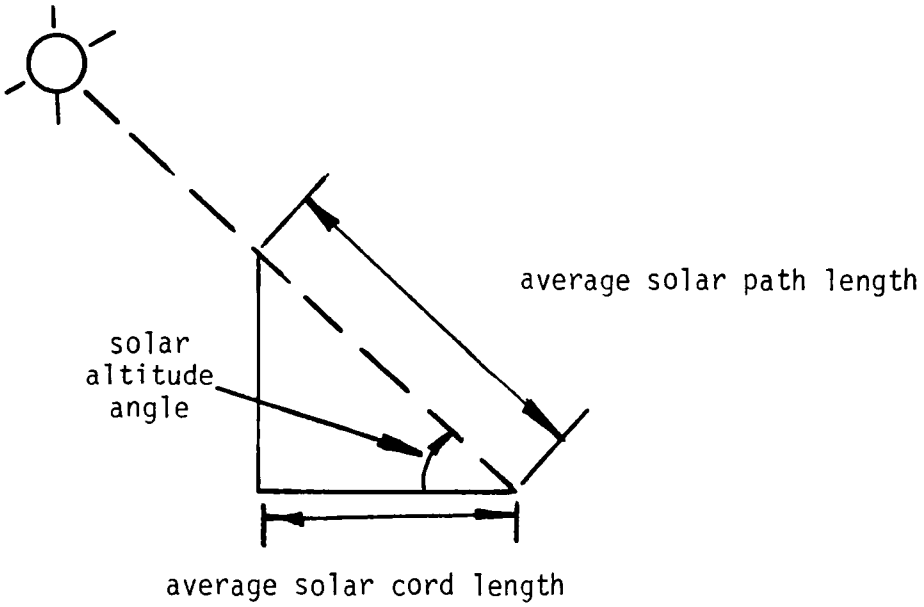


Figure 10. Approach used to determine average path length traveled in the tube

absorbed is linear over the magnitude of extinction coefficients in the visible spectrum.

The total energy passing through the tube was calculated by inserting the average cord length into Equation (4) and multiplying that amount by the transmittance of the fiberglass at angle of incidence of 60 degrees.

The radiation exchange between the tube and the glazing was modeled as a two-body enclosure. The equation for a two-body radiation exchange is given below:[33]

$$q_{1-2} = \frac{E_{b1} - E_{b2}}{\frac{1 - \varepsilon_1}{\varepsilon_1 \cdot A_1} + \frac{1}{A_1 \cdot F_{1-2}} + \frac{1 - \varepsilon_2}{\varepsilon_2 \cdot A_2}} \qquad (5)$$

Figure 11 shows how the radiation exchange was viewed, the areas involved, and how Hottel's string method was used to calculate the shape factors. The black body emissive power shown in Equation (5) as E_b can be written as:

$$E_b = \sigma \cdot \dot{T}^4 \qquad (6)$$

This allows the numerator of Equation (5) to be written as:

$$E_{b1} - E_{b2} = \sigma \cdot (\dot{T}_1^4 - \dot{T}_2^4) \qquad (7)$$

The right side of Equation (7) can be factored to give:

$$\sigma \cdot (\dot{T}_1^2 + \dot{T}_2^2) \cdot (\dot{T}_1 + T_2) \cdot (\dot{T}_1 - T_2) \qquad (8)$$

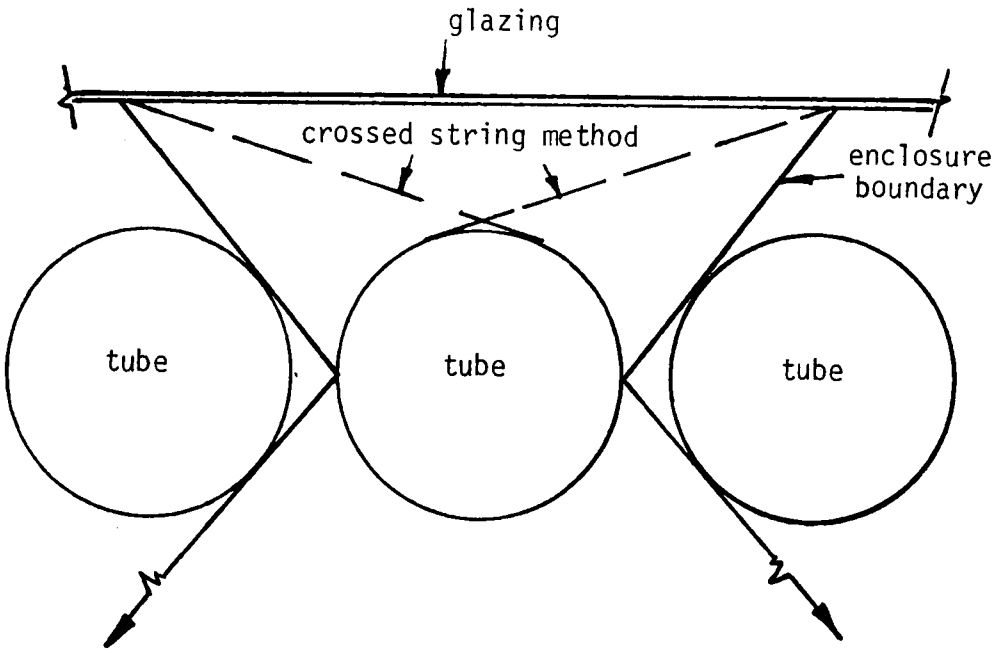


Figure 11. Radiation exchange between a tube and its surroundings

The problem was linearized by defining h_r as a radiation heat transfer coefficient, as shown in Equation (9):

$$h_r = \sigma \cdot (\dot{T}_1^2 + \dot{T}_2^2) \cdot (\dot{T}_1 + \dot{T}_2) \qquad (9)$$

Temperatures from the previous time-step are used to solve Equation (9). The radiation energy balance for the two-body enclosure can then be written as:

$$q_{1-2} = \frac{h_r \cdot (\dot{T}_1 - \dot{T}_2)}{\text{DENOM}} \qquad (10)$$

where DENOM is the denominator of the right-hand side of Equation (5).

As shown in Figure 11, the tube sees two surfaces that are different than its own. The south glass or night insulation can be a great deal colder than the north wall (an interior wall) of the room containing the tubes. For this reason, Equation (5) was applied twice, once to an idealized enclosure on the south side of the tube and once to an idealized enclosure on the north side of the tube.

A diameter-to-height ratio of 0.143 allowed the tube convection losses to be modeled using the equations for a flat vertical wall. The convection was defined as either laminar or turbulent, and the appropriate constants were applied to the empirical equation below:[33]

$$\overline{Nu} = \frac{\overline{h}_c L}{K_f} = C \cdot (Gr_f \cdot Pr_f)^a \tag{11}$$

The average Nusselt number determined in Equation (11) was used to solve for the natural convection coefficient. The energy balance on the tube was then written as:

$$MC_p \frac{dT}{dt} = A_{TN} \cdot h_{rN} \cdot \frac{(T_{wall} - T_{tube})}{DENOMN} + A_{TS} \cdot h_{rS} \cdot \frac{(T_{glass} - T_{tube})}{DENOMS} + h_c \cdot A_{TT} \cdot (T_{room} - T_{tube}) + Q_{solar} - Q_{thru} \tag{12}$$

The change in temperature in Equation (12) was assumed to be independent of all factors except time; therefore, change with respect to time was written as $\frac{dT}{dt}$, and Equation (9) was written as:

$$\frac{dT}{dt} = A_{TN} \cdot h_{rN} \cdot \frac{(T_{wall} - T_{tube})}{DENOMN} + A_{TS} \cdot h_{rS} \cdot \frac{(T_{glass} - T_{tube})}{DENOMS} + A_{tube} \cdot h_c \cdot (T_{room} - T_{tube}) + (Q_{solar} - Q_{thru})/MC_p \tag{13}$$

This differential equation was solved by TRNSYS using a Modified-Euler numerical integrator. The old value of tube temperature was automatically replaced in the program by the new value. After the new tube temperature was calculated, the new amount of energy stored in the tubes and the mean radiant temperature (MRT) were calculated.

The MRT was calculated using the approach outlined by Fanger.[3] Fanger developed the following relationship based upon his definition of MRT (see page two):

$$\varepsilon_p \cdot \sigma \cdot (\dot{T}^4_{MRT} - \dot{T}^4_{CL}) = \varepsilon_p(J_1F_{p-1} + J_2F_{p-L} \cdots\cdots J_nF_{p-n}) - \varepsilon_p \qquad (14)$$

Equation (14) was solved for the MRT to give:

$$\dot{T}^4_{MRT} = \frac{1}{\sigma} \cdot (J_1F_{p-1} + J_2F_{p-2} \cdots\cdots J_nF_{p-n}) \qquad (15)$$

Fanger made the assumption that all surfaces in the room were black. This approximation was made because the emittance of most building materials is 0.9. By substituting $\sigma \cdot \dot{T}^4_n$ (black body emissive power) for J_n in Equation (15), Equation (16) was developed as follows:

$$\dot{T}^4_{MRT} = \dot{T}^4_1F_{p-1} + \dot{T}^4_2F_{p-2} + \cdots\cdots + \dot{T}_nF_{p-n} \qquad (16)$$

A final condition that all temperatures in the room must be close together allowed Fanger to linearize Equation (16) to give the final form for T_{MRT}:

$$T_{MRT} = T_1F_{p-1} + T_2F_{p-2} + \cdots\cdots + T_nF_{p-n} \qquad (17)$$

Equation (17) states that the mean radiant temperature of a point in a room is the mean value of the surrounding surface temperatures weighted by the magnitude of their respective shape factors.

Graphs prepared by Fanger (derived from experiments on human subjects) were used to determine shape factors between an adult sitting at any orientation in the center of the living room of the passive modular house and the various surfaces with different wall temperatures in that room. The shape factors between the subject and the combined area of all of the water tubes in the living room were determined to be 0.058. A complete development of these shape factors between an individual in the room and the south wall can be found in Appendix D.

Heating Load Calculation

The TRNSYS room model summed the solar input, internal generation, conduction losses or gains, and infiltration losses or gains. The space heating load in this mode of operation was defined as the amount of auxiliary energy required to counteract heat losses and hold the room temperature above a minimum value. The building temperature never fell below the lower limit because it was assumed that the back-up heat could exactly meet the load. This was a reasonable assumption for the passive modular house since the back-up heat is electrical resistance baseboard type.

A new room temperature was calculated whenever the auxiliary energy requirement was positive. (Recall that heat loss is negative; thus, a heating load is negative and a cooling load is positive.) This single-mode temperature was calculated by the expression given in Equation (18) below:

$$\frac{dT}{dt} = \frac{Q_{load}}{capacitance} \qquad (18)$$

Equation (18) was solved in TRNSYS by assuming that the change in temperature with respect to time was linear over the time-step used in the program. This allowed the equation to be written as:

$$T_{new} = T_{old} + \frac{Q_{load} \cdot \Delta t}{capacitance} \qquad (19)$$

The building capacitance used in this equation was defined by TRNSYS to be the capacitance of the building structure and its contents. While this is difficult to estimate for most houses, this was not the case for the passive modular house because the house weight was known, and it contained no furniture.

The mass of the structure, approximately 29,000 kg, was multiplied by an average value of specific heat taken from the major building materials. The capacitance of the water in the tubes and air in the house was calculated at 20°C. These three capacitances were summed to give a value of 39,000 kJ/°C, the total capacitance used in the program.

Inputs from the models described in previous sections were fed into the load subroutine. Internal generation was set equal to zero since the house was unoccupied, and other sources of internal generation, such as appliances or hot water heaters, were not in use. The TRNSYS space heating load model required specifying the infiltration rate as a constant number of air changes per hour. This approach has been shown to cause significant errors in the calculation of hourly heating loads.[34]

Another technique used by designers to estimate infiltration rates is the crack length method. The driving force for infiltration is known to be a pressure and temperature difference between the inside and

outside air. The pressure differences are caused by wind striking the structure. Unfortunately, a basic understanding of these driving forces alone does not make the calculation of the rate easy. A knowledge of the total crack length, width, and distribution throughout the building, as well as the pressure distribution, is required to calculate the infiltration rate from the basic principles. Collection of this information for use in the crack length method usually is not justified due to inaccuracies in the rate calculated arising from limited information of air leakage characteristics of the various openings.[20] In addition, studies have shown that visible cracks, such as those around windows and doors, accounted for less than 25 percent of the total cracks in a house.[35]

For these reasons, researchers have been experimentally determining infiltration rates for several years.[35] Out of this experimental work has come a series of expressions relating infiltration rates to wind velocity, inside and outside temperature difference, and building construction. Peterson has reviewed several of these works and provides empirical equations representing a consensus on the relationship between infiltration rate, building construction, and the driving forces, as shown below:[35]

$$In_{total} = AA + CC \cdot \Delta T + DD \cdot V_w \qquad (20)$$

The constants CC and DD in Equation (20) have been determined to fall between 0.006 to 0.012 and 0.15 to 0.030, respectively. The constant AA was given a value of 0.1 by Peterson. Unfortunately, the problem of determining the effect of tightness of building construction on the rate of infiltration is still present in this approach because the values of

CC and DD are assigned by assessing this building quality. However, if these coefficients can be determined by experimental verification, a good means is provided to increase agreement between predicted and actual values of the infiltration rate, thus improving the accuracy of hour-by-hour predictions of auxiliary energy requirements. Figure 12 illustrates the great impact the infiltration rate has on the heating requirements of a house.

A final change to the load calculation model was the addition of a code to simulate a crawl space. The decision was made to model the heat transfer through the floor by the UA method since the temperature difference across the floor did not vary rapidly with time. The major challenge in this portion of the work lay in predicting the crawl space temperature: quoting ASHRAE, "Temperature in crawl spaces may vary widely. . . . It is necessary, therefore, to evaluate the conditions and select an appropriate temperature by judgment."[20] Based upon personal observation at a residence with similar crawl space in Blount County, the crawl space temperature was predicted by the equation shown below:

$$T_{CR} = (T_{CR} + T_A)/2 \qquad (21)$$

The ground temperature was assumed to be constant. The value used was 15.6°C. This value was an average of measured values of soil temperature taken at the TECH site in the vicinity of the passive house. An accurate determination of the crawl space temperature and infiltration rate during the heating season in the passive modular house must wait until winter data are available.

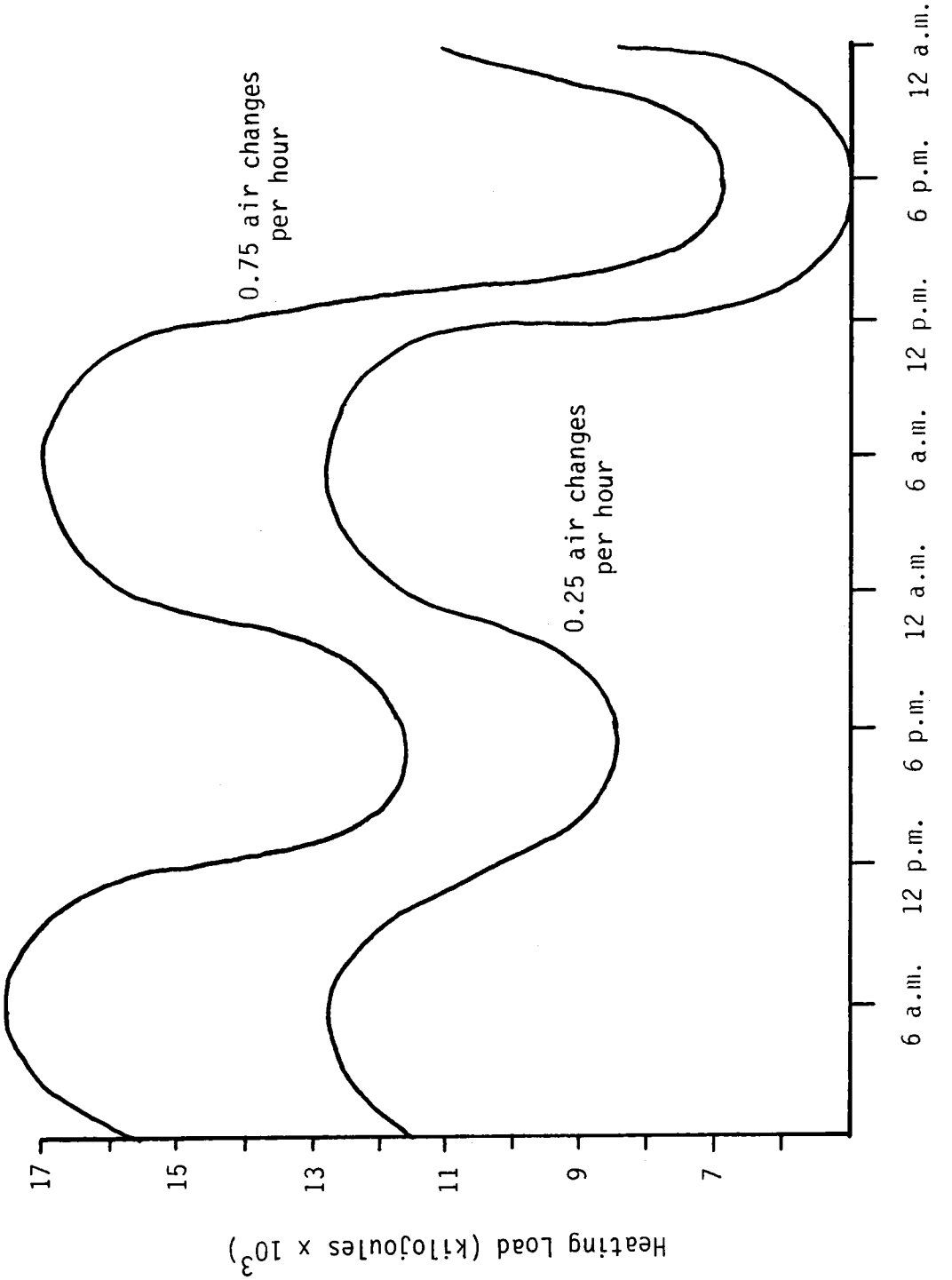


Figure 12. The influence of infiltration rates on building heating requirements.

Solar Radiation Models

Total solar radiation is measured at the TECH site on a 45-degree slope. The measurement is averaged for one hour and is then stored as a single reading at the beginning of that hour. The TRNSYS radiation processor requires total radiation on a horizontal surface. In order to determine a value for the total radiation on a horizontal surface, a TRNSYS subroutine was written using the iterative technique developed by Pawelski.[25]

The total instantaneous radiation incident on a tilted surface is as follows:

$$H_T = H_b R_b + H_d \cdot \left(\frac{1 + \cos(S)}{2}\right) + (H_b + H_d) + \rho \cdot \left(\frac{1 - \cos(S)}{2}\right) \qquad (22)$$

The source of the various components of H_T in Equation (22) is shown in Figure 13 below.

Figure 13 illustrates that the total radiation on the tilted surface is the sum of the beam and diffuse radiation that directly strike the surface, plus the beam and diffuse radiation reflected from the ground that strikes the surface. This assumed that the fraction of diffuse radiation incident on the surface from the sky was equal to the view factor, 1 + COS(S)/2, between the surface and the sky times the diffuse component of radiation. This assumption is correct when the diffuse radiation is isotropic and the view between the receiver and sky is unobstructed.

Before an iterative loop was begun, the instantaneous extraterrestrial radiation per unit area on a horizontal surface was calculated using the relationship shown in Equation (23) as given by Duffie and Beckman:[36]

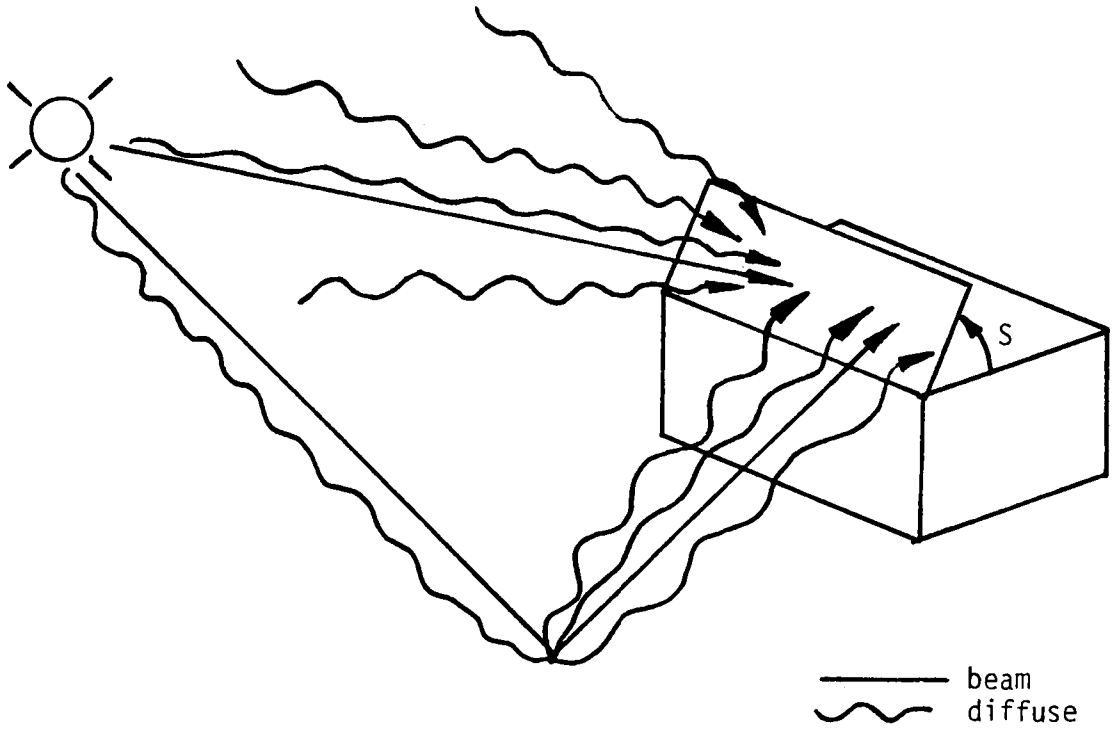


Figure 13. Beam and diffuse radiation striking a tilted surface

$$H_o = [1 + 0.033 \cdot \cos(360 \cdot nd/365)] \cdot S_c \cdot \cos(\theta_H) \qquad (23)$$

An initial guess of the instantaneous solar radiation on a horizontal surface was made by letting $H = 0.5 \cdot H_o$. The ratio of horizontal to extraterrestrial radiation, KT, is then 0.5.

A correlation by Lui and Jordan relating diffuse and total radiation was used to split the guessed value of total radiation.[36] Equations (24) and (25) show this process.

$$H_d = H(1.0045 + 2.6313 \cdot KT^3 - 3.5227 \cdot KT^2 + 0.0049 \cdot KT) \qquad (24)$$

$$H_b = H - H_d \qquad (25)$$

R_b, defined as the ratio of instantaneous beam solar radiation intercepted by the tilted surface to the instantaneous beam solar radiation intercepted by a horizontal surface, was next calculated using geometric relationships between the two surfaces and the sun. This term can be calculated by dividing the cosine of the angle of incidence for the tilted surface by the cosine of the angle of incidence for the horizontal surface.

Equation (22) was divided by H to give Equation (26), shown below:

$$R = \frac{H_T}{H} = \frac{H_b}{H} \cdot R_b + \frac{H_d}{H} \cdot \left(\frac{1 + COS(S)}{2}\right) + \rho \cdot \left(\frac{H_b + H_d}{H}\right) \cdot \left(\frac{1 - COS(S)}{2}\right) \qquad (26)$$

All the quantities on the right-hand side of Equation (26) could be calculated because of the $H = 0.5 \cdot H_o$ estimate. A new value of H was then calculated by dividing H_T by R. Finally, H new was compared to H old. When the difference between these two quantities was less than 50 kJ/Hr, the iteration was stopped. This limit on the iteration was approximately 1.5 percent of the midday radiation measured by the pyranometer at the TECH site on a bright January day during the winter of 1980-1981. The logic used in this subroutine is illustrated in Figure 14.

The calculated value of total radiation on a horizontal surface was sent to the TRNSYS radiation processor. The processor then split this value into its beam and diffuse components using a correlation developed by Boes.[38] The Boes correlation has been experimentally shown to be one of the most accurate methods available for determining the components of total radiation.[39]

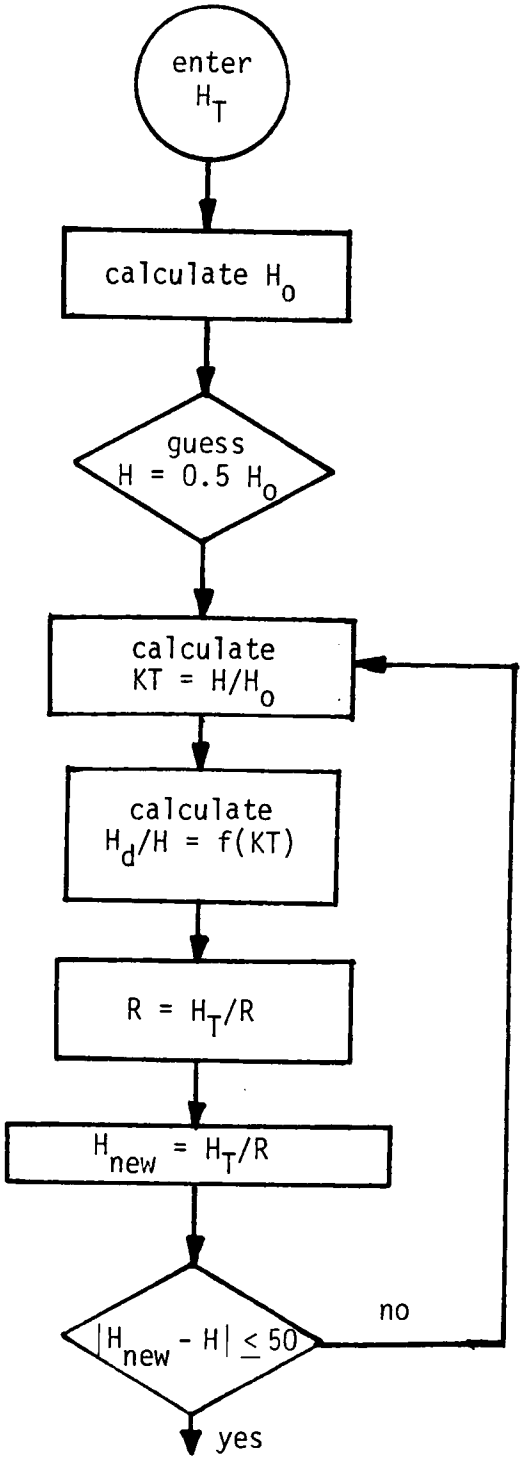


Figure 14. Radiation convertor logic

The values of radiation calculated by TRNSYS were instantaneous values of solar intensity. These values were calculated for the midpoint of each hour and assumed constant for that entire hour.

Component Configuration

TRNSYS subroutines were linked together to receive and send information. The first unit in this process was the data reader. This reader took information from the data tape each time-step (usually one hour) and converted it to the units used in the other subroutines. The items read each hour were:

1. Total solar radiation per unit area per unit time (either on a horizontal or tilted surface)
2. Dry bulb temperature
3. Wind speed
4. Wind direction

Solar radiation was processed as described in the previous section and was then sent to the wing wall and overhang subroutine. One of these subroutines was set up for the windows in each of the three south-facing rooms. The three average solar intensities generated by the wing wall-overhang subroutine were summed and then sent to the window subroutine. This subroutine modeled the south-facing glass as a single unit. A forcing function subroutine acting as a timer told the window subroutine whether or not the shades were down. The amount of solar radiation transmitted by the glass when the shades were up was sent to the Kalwall tube model. In this model, the amount of radiation transmitted, reflected, absorbed, and not striking the tubes was calculated.

These solar inputs, plus the heat loss by the tubes, were sent to the load calculator.

In conjunction with the above calculation, the window model, wall models, and attic model were calculating conduction heat losses. These models received room temperatures from the load model and ambient temperature from the data reader. In addition, non-south-facing wall models calculated the radiation gains and conduction losses for any windows in their respective sides. All conduction heat losses (or gains) were summed and sent to the load model, as well as radiation gains from non-south-facing glass. The load calculator then predicted the heat loss through the floor and summed all losses and gains. If the new room temperature was above the lower limit specified by the user, an iterative solution would begin. Each output that varied with room temperature was recalculated by using successive substitution. This process continued until the old and new values of each output being recalculated were within a user-specified tolerance.

After iteration was completed during each time-step, values specified by the user were sent to a quantity integrator for summing over the length of the simulation. These values were then sent to a printer for computer output. Figure 15 is a block diagram showing this information flow.

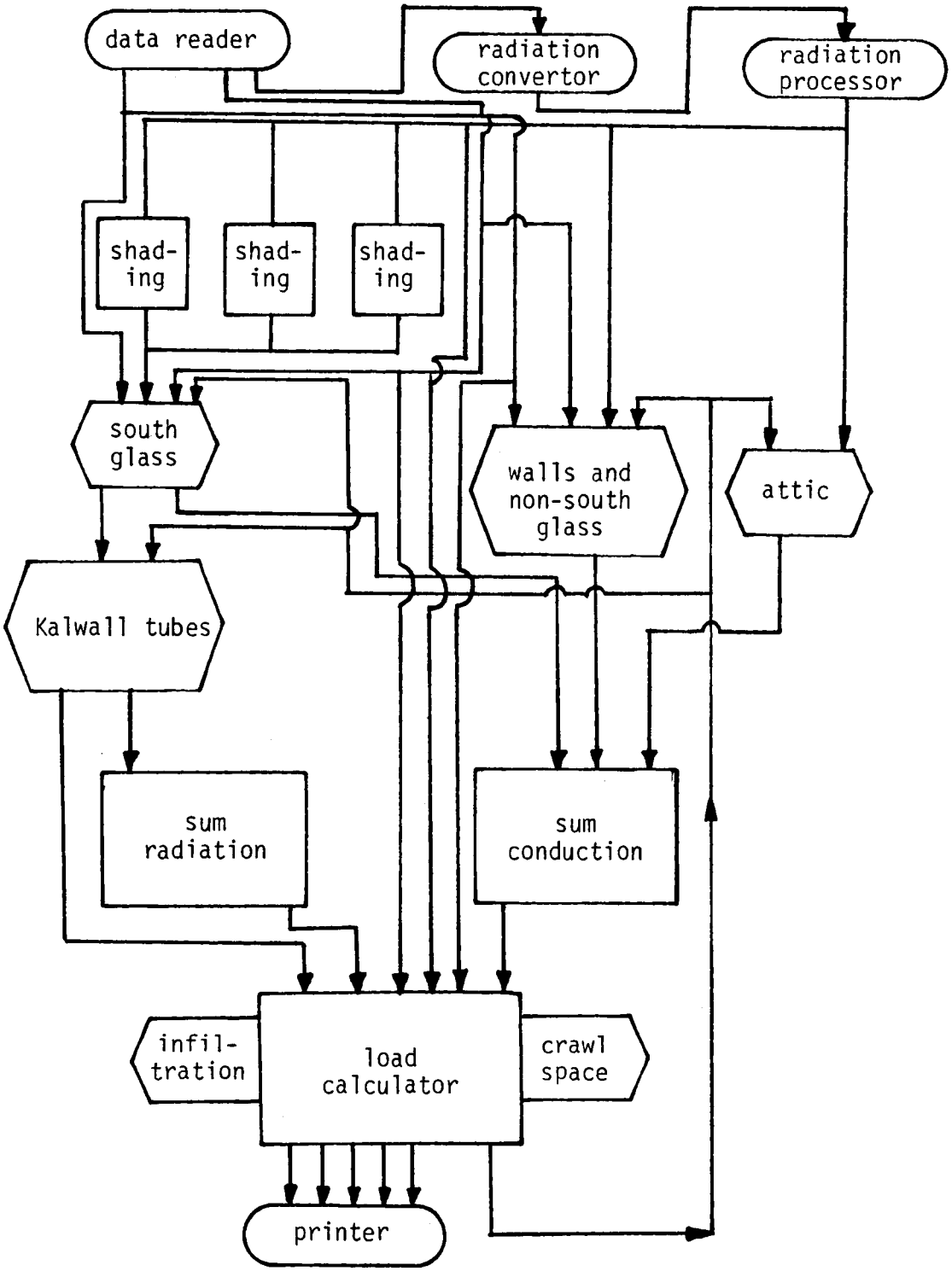


Figure 15. TRNSYS component configuration

CHAPTER III

EXPERIMENTAL VALIDATION

Two computer models developed for this study were experimentally verified. Solar radiation measured at an angle by TVA at a test facility in Chattanooga, Tennessee was used to verify the radiation convertor by comparing its calculated values of total radiation on the horizontal with horizontal values measured at the Chattanooga site. Dake and Harleman's equation used to calculate the amount of solar energy transmitted through water was verified independently of the tube model, with experiments carried out at the passive solar house. In addition, the tube temperature predicted by the Kalwall model was compared to measured values to determine the accuracy of the entire tube model.

The passive modular house was delivered to the TECH site on April 1, 1981. This late delivery precluded any house model verification tion under winter conditions. It was felt that supplying experimental verification of the passive heating system (i.e., the entire house model) with data measured during the month of May would do little to enhance the model's credibility. This conclusion is supported by the fact that unverified portions of the house model, such as the infiltration rate and crawl space temperature, are highly weather dependent and will vary a great deal from season to season. In addition, sun angles and subsequent shading problems encountered in the winter differ greatly from those seen in the spring.

Determination of Extinction Coefficient for Water

A pivotal part of the energy balance on the Kalwall tubes was the prediction of the total amount of energy absorbed and transmitted by the water. The equation used for this calculation in the tube model contained two parameters (see Equation (4), page 23): β, the fraction of radiation absorbed at the water's surface; and K, the extinction coefficient of the water. Recall that β accounted for the complete absorption of infrared radiation by water in the first few centimeters of depth. Dake and Harleman concluded that β had a value of 0.4 and K a value of 0.05 m^{-1}.[32] A review of the literature turned up little information addressing these parameters. It was noted, however, that approximately 40 percent of the solar spectrum is in the infrared region (0.9×10^{-6} m and above). This supported the choice of 0.4 for β. An examination of the extinction coefficient for water in the visible range showed it to be highly variable with wave length. This was a marked departure from the assumption of constant optical properties across the solar spectrum made for materials in this model. Between the wave lengths of 0.4×10^{-6} m and 0.7×10^{-6} m, the extinction coefficient for water increased by more than a factor of ten. Using a constant path length of 0.305 m, the highest and lowest values of K caused a 15 percent change in the amount of light transmitted by water. An additional point of concern lay in the fact that Dake and Harleman's work was conducted on lakes, while the Kalwall tubes were filled with tap water.

For these reasons, an experiment was prepared to determine an average value for K across the visible spectrum under the actual conditions of the passive house. Two silicon cell pyranometers were placed

behind the same Kalwall tube partially filled with water. The bottom pyranometer was behind the portion of the tube that was filled with water, while the top one was behind the empty part of the tube. The water depth was such that the average path length of radiation through the water remained near 0.305 m while the sun moved through the sky. Figure 16 shows the placement of the instruments behind the tube. The pyranometers were sealed so that they only received radiation which had passed through the tube. The difference between the readings of the two pyranometers was recorded on a strip chart recorder.

A total of 25 readings was taken from five days of data. These five days represented a variety of weather conditions. The readings were put into the equation for solar transmission as the values of I(0) and I(L). The value of L was 0.305 m, and β was 0.4 m. Solving Equation (4) for $\bar{k}$ yields:

$$\bar{k} = \ln \left(\frac{I(L)}{I(0)}\right) \cdot \frac{1}{-0.305} \qquad (27)$$

The mean value of 25 solutions to Equation (27) was 0.60 m^{-1}. The standard deviation of this mean value was found to be 0.096 m^{-1}.

The magnitude of this experimentally derived value generated some concern since it was over ten times larger than the value of 0.05 m^{-1} used by Dake and Harleman. One must be cognizant of the fact that, as previously noted, the two experiments were carried out under widely varying conditions. The value arrived at in this study should not be thought of as an extinction coefficient for water, but merely as an empirical constant in an equation. A final fact worth noting is that the ratio of the two values measured in experiments at the passive

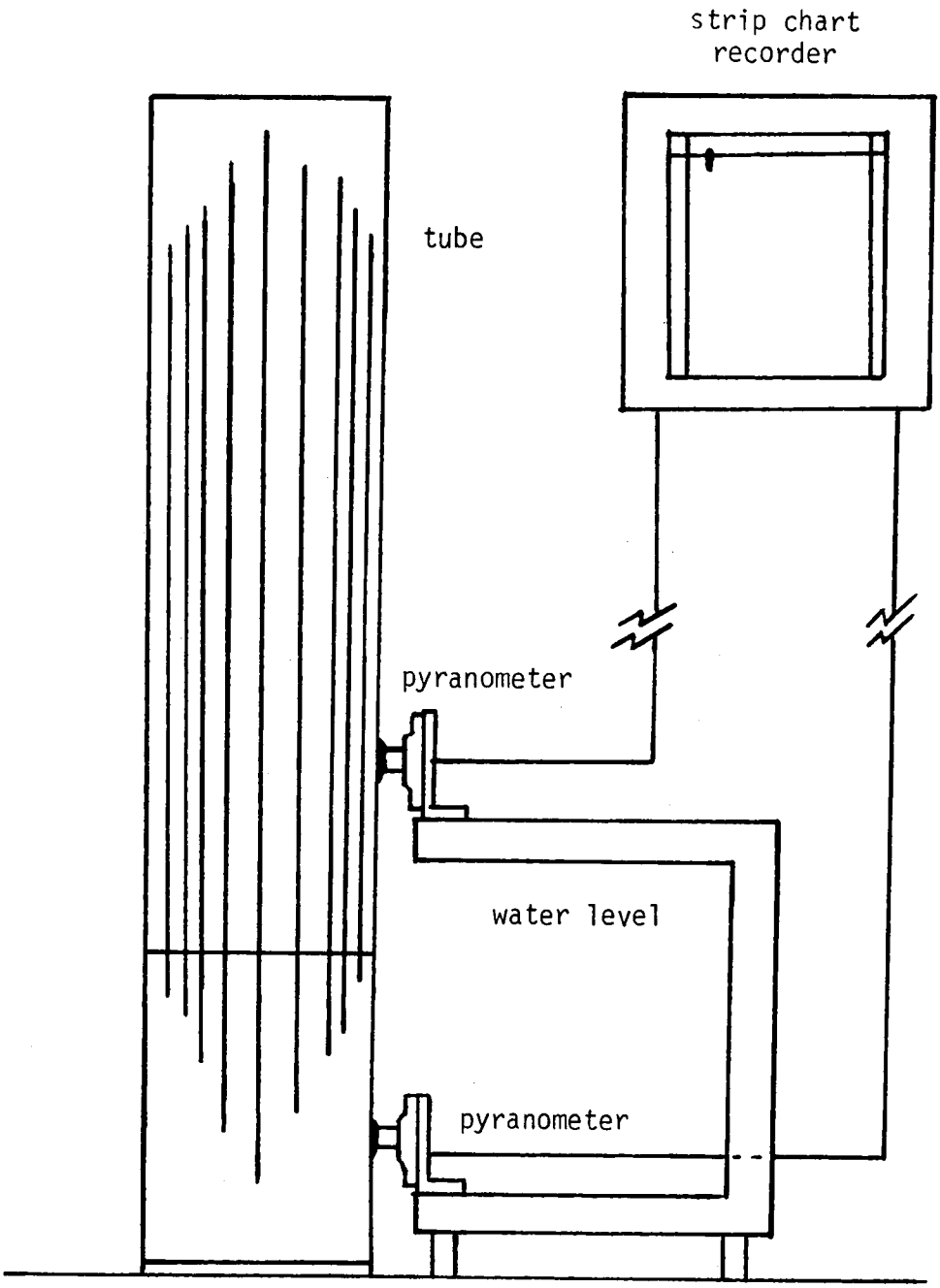


Figure 16. Equipment layout for the experimental determination of the amount of sunlight trapped by the water in a Kalwall tube

modular house, I(L)/I(0), does not differ drastically from the calculated value of this ratio using Dake and Harleman's value of 0.05 m^{-1} at a depth of 0.305 m. This is illustrated by solving Equation (4) for I(L)/I(0), using L = 0.305 m and the values of 0.05 m^{-1} or 0.6 m^{-1} for K. Letting K equal 0.05 m^{-1} gives a ratio of 0.59, while 0.6 m^{-1} gives a ratio of 0.50.

Validation of the Radiation Convertor

The data supplied by TVA contained total radiation measured on the horizontal and at an angle of 35 degrees from the horizontal. These data provided the opportunity to validate the radiation convertor used to transform measured total radiation on an angle of 45 degrees (as measured at the TECH site) to the horizontal (as required by TRNSYS). Values of total radiation on the horizontal were calculated from the data measured at 35 degrees and compared to the actual data on the horizontal for a period of one week. The average hourly value of measured radiation on a horizontal surface during daylight hours of this period was 1513 kJ/m^2. The standard deviation of the predicted value from the measured value for this validation period was calculated to be 82.9 kJ/m^2. Dividing this value by the average measured value gave a normalized standard deviation of 5.5 percent. Figure 17 shows a plot of measured and calculated radiation on the horizontal for a typical 24-hour period.

Validation of the Kalwall Tube Model

Tube water temperatures, room temperature, ambient weather conditions, and solar radiation were recorded at the passive modular house

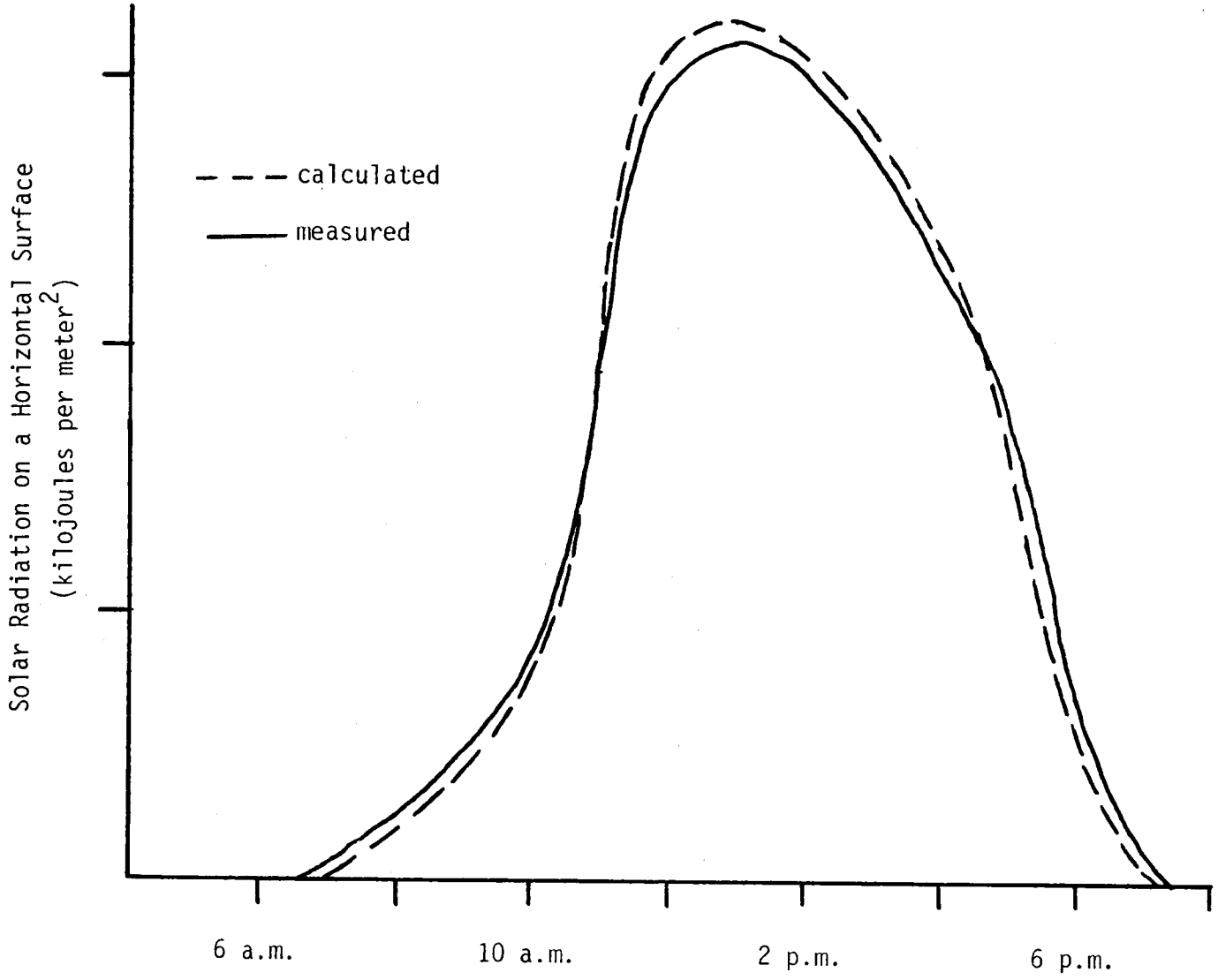


Figure 17. Comparison of calculated and measured radiation on a horizontal surface for the day of March 31, 1981. Measured data collected in Chattanooga, Tennessee.

for the period from April 15, 1981 to May 18, 1981. The first use of this measured data was to examine the validity of assuming that thermal stratification could be neglected and that all of the tubes were nearly the same temperature. Sensors were placed 0.15 m from the top and bottom of three tubes in the house. The maximum top-to-bottom difference in any one tube never exceeded 2.12°C during the 95-hour period examined. The average temperature difference during this 95-hour period amounted to less than 3.2 percent of average tube temperature during that same period. A comparison of temperatures at the same height in two separate tubes in two different rooms of the house over a 24-hour period showed a maximum temperature difference of 0.31°C at any one time. This is explained by the fact that buildings on either side of the passive modular house caused the western tubes to heat up earlier in the day than those further east. However, this phenomenon is reversed in the evening, and the western-most tubes are shaded first. Since the cycle evens itself out, a typical 24-hour average of the hourly temperature differences between these same two tubes was only 0.12°C. The conclusion from this examination was that using a representative tube at a constant temperature throughout to model the 20-tube system was a good method.

The major validation work for this computer simulation was in the comparison of the predicted and measured tube temperatures. For this validation, a 21-day-long data tape was prepared containing measured values of ambient temperature, tube temperature, room temperature, and solar radiation. The 21-day period represented the longest period of time data were collected without interruption. The measured solar

radiation was processed by the radiation convertor, wing wall-overhang model, and the window model before it was fed into the Kalwall tube model. The tube model also received values of measured room temperature and calculated south glass temperature. The north wall of all rooms containing tubes was an interior wall and assumed to be at room temperature. Figure 18 shows a block diagram representing the interconnection of subroutines for the tube model verification.

The tube model verification program took the difference between the calculated tube temperature and the average of the measured top and bottom temperatures of one tube for 504 hours. These differences were used to calculate a standard deviation which was found to be 0.533°C. This value was divided by the average measured value of tube temperature, 23.43°C, to give a value of normalized standard deviation of 2.27 percent. Figure 19 shows a plot of measured and calculated tube temperatures for a period of 24 hours.

Using the term "accuracy" to signify the normalized standard deviation, it must be noted that a judgment of the accuracy of the tube model was limited by the less accurate radiation convertor, which had a normalized standard deviation of 5.5 percent.

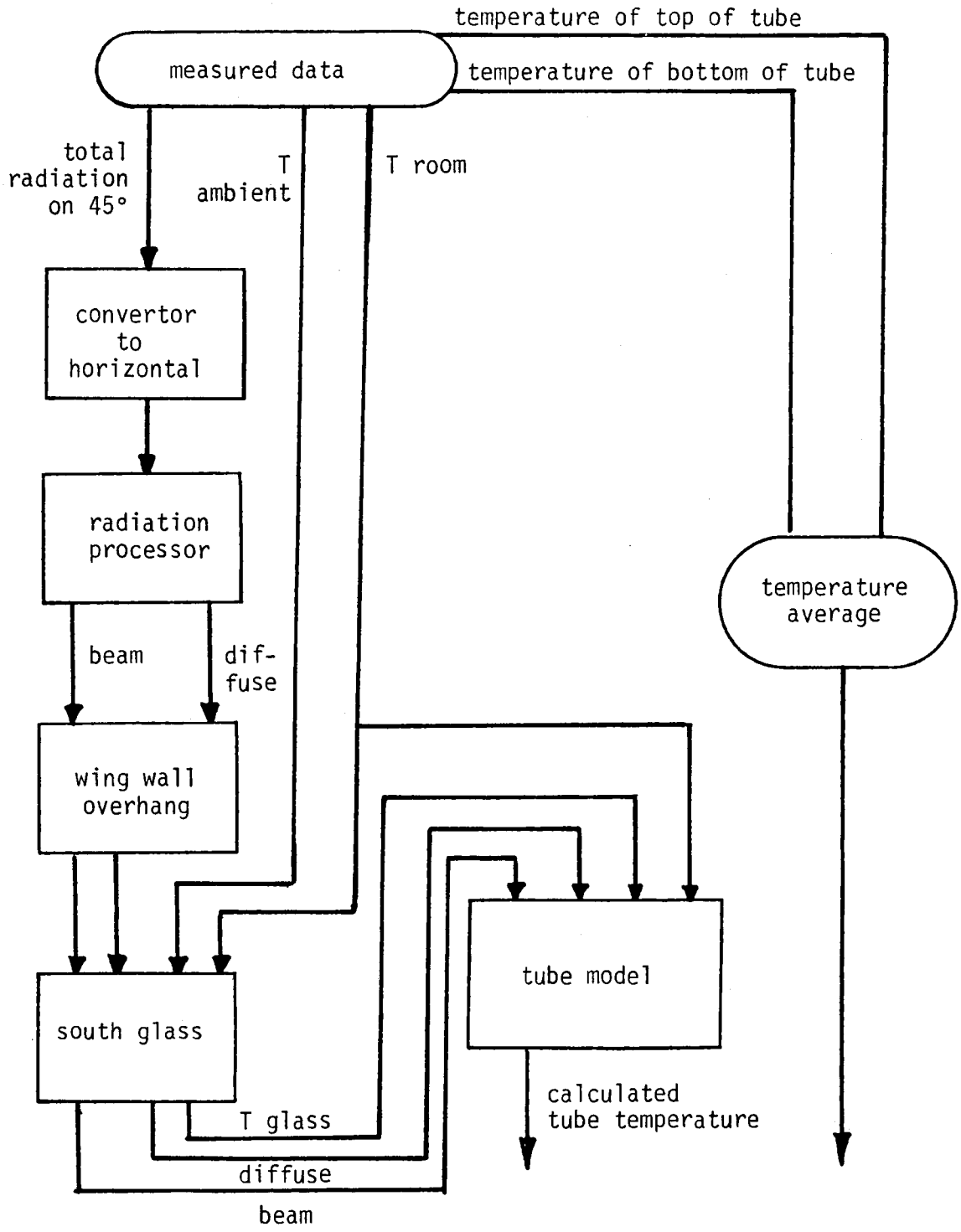


Figure 18. TRNSYS component configuration for tube model verification

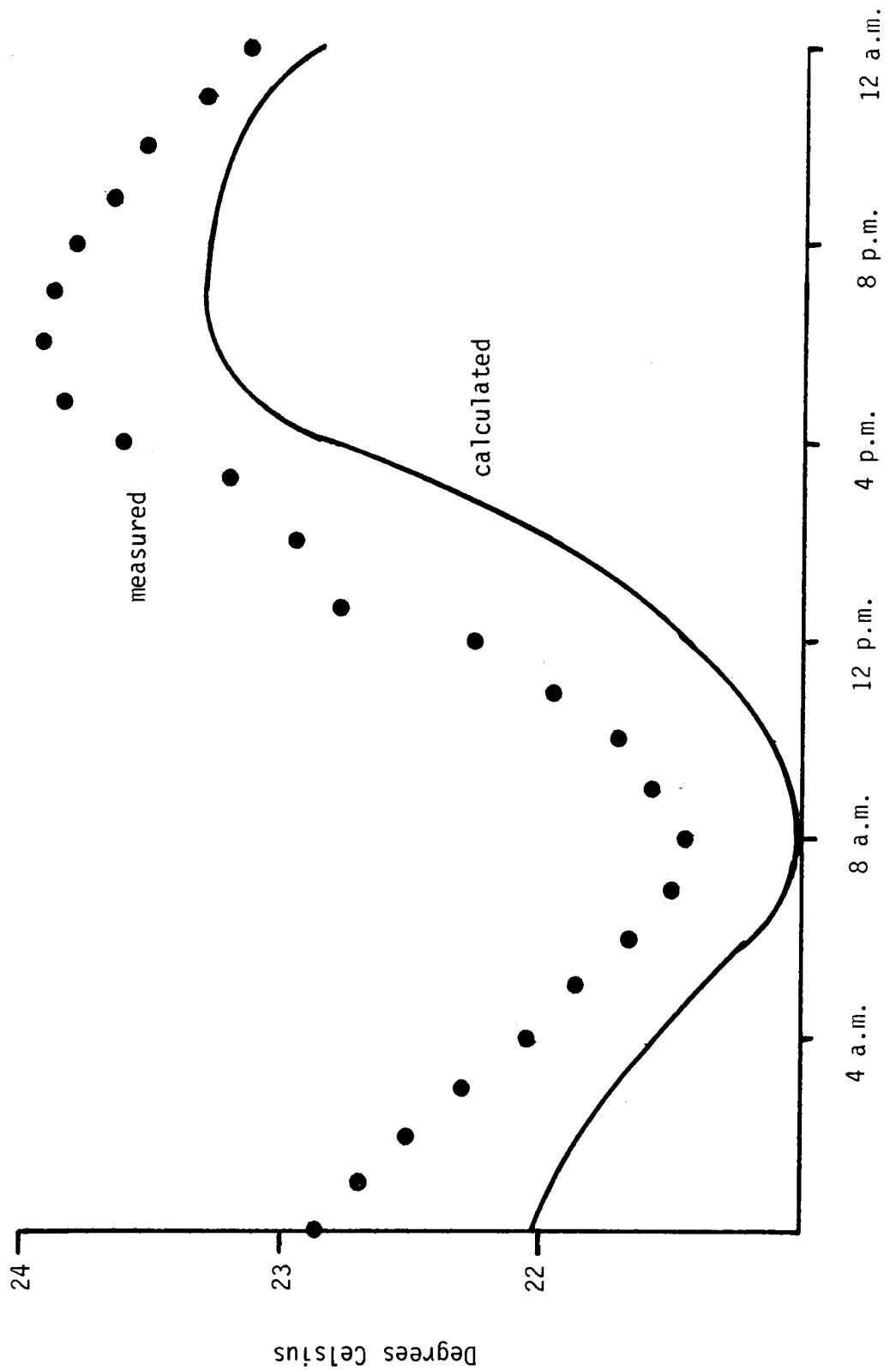


Figure 19. Measured and calculated tube temperatures for April 22, 1981

CHAPTER IV

HEATING SEASON SIMULATION RESULTS

Heating Season Weather Data

The performance of the passive modular house was simulated for an entire heating season. The weather data used for these simulations was a Typical Meteorological Year (TMY). The TMY is a collection of typical weather months from the period for most National Oceanic and Atmospheric Administration (NOAA) weather stations. The typical months were chosen by a statistical procedure which examined the variance of certain indices for a particular month from the long-term average. Some parameters, such as solar radiation, were weighted more heavily than others during this evaluation.[40]

The premise of a typical weather year has been tested by Freeman.[41] In this study, the results from an active solar heating and cooling system using the TMY and average results from the same system run for all of the years available (usually 20-25) were shown to compare favorably.

The NOAA weather station closest to the TECH site is approximately seven miles to the south at the Knoxville Airport. This particular reporting station does not measure solar radiation directly. The insolation data for stations where these measurements are not made were correlated from cloud cover data. These correlations, developed by NOAA, have been found to generally predict solar radiation within five percent of measured values.[42]

Alternative Systems Performance

In addition to modeling the passive house as it was constructed, the house was modeled with the following alterations:

1. Night insulation removed.
2. Water tubes removed.
3. Water tubes and night insulation removed.
4. South glass reduced from 14.66 m^2 to 7.21 m^2 and night insulation removed. This model is considered to be a conventional house.
5. Water tubes increased by 20 percent.

All simulations in this comparison had no internal generation. In all cases, Kimura's relationship between wind velocity and outside convection coefficient was used. Also, the infiltration rate was kept as a weather dependent variable throughout the work, as described in Chapter II.

The heating season used for these simulations began October 1 and ran for 31 weeks, ending on April 30. This 5,280-hour-long period was chosen to include all dates when the temperature fell below 10°C.

Table 1 summarizes the results of these simulations. The version of the passive solar house that was installed at the test facility required less auxiliary energy than any other design, while the conventional house required more back-up heat than any other variation.

The Impact of Night Insulation

As shown in Table 1, covering the large expanse of south glass with an insulating window shade each night caused a reduction in auxiliary energy requirements of 24 percent. For these simulations, the

TABLE 1

COMPARISON OF PASSIVE SOLAR ALTERNATIVES FOR A HEATING SYSTEM

Passive Modular House Alternative	Auxiliary Heat Required (kJ)	Heat Gained Through South Glass (kJ)	Heat Lost Through South Glass (kJ)	Net Heat Gain Through South Glass (kJ)
1--As Installed	7.670×10^6	2.526×10^7	5.754×10^6	1.951×10^7
2--With 20 Percent More Water Tubes	7.393×10^6	2.526×10^7	5.749×10^6	1.951×10^7
3--With No Night Insulation	1.004×10^7	2.526×10^7	9.757×10^6	1.550×10^7
4--With No Tubes	8.487×10^6	2.526×10^7	5.738×10^6	1.952×10^7
5--With No Tubes or Night Insulation	1.108×10^7	2.526×10^7	9.770×10^6	1.549×10^7
6--With Reduced Glass and No Night Insulation (Control House)	1.411×10^7	1.283×10^7	4.597×10^6	8.233×10^6

insulating shades were drawn when total solar radiation striking the glass was less than 50 kJ/m^2. This was an arbitrary selection, which was roughly equivalent to sundown. The shades were opened each morning at 7:00 a.m.

Table 1 shows that the south-facing glass had a net energy gain even without the use of night insulation. The value of this net gain can be deceiving because 47 percent of this amount occurred during the first and last six weeks of the TMY when the ambient temperature was less severe. During two weeks of the simulation, one in December and one in January, the glass actually lost more energy from conduction than it gained through solar radiation.

The Impact of Storage

The passive house as installed at the TECH site required 10 percent less auxiliary energy than the version with no tubes. The model with no tubes overheated when the sun was bright and the ambient temperature was above approximately 12°C. On the other hand, the version with tubes did not overheat until the ambient temperature rose above approximately 19°C on a bright sunny day. For the purposes of this study, overheating was defined as the point when the room temperature rose above 24°C. At this time, it was assumed that the house would be ventilated and, therefore, would not exceed the 24° limit. The house without tubes overheated 597 hours during the heating season, while the version with tubes only overheated 523 hours.

Figure 20 illustrates the function of the tubes during less sunny weather, when overheating was not a problem. The period shown is from the first week in January. The passive alternative containing tubes

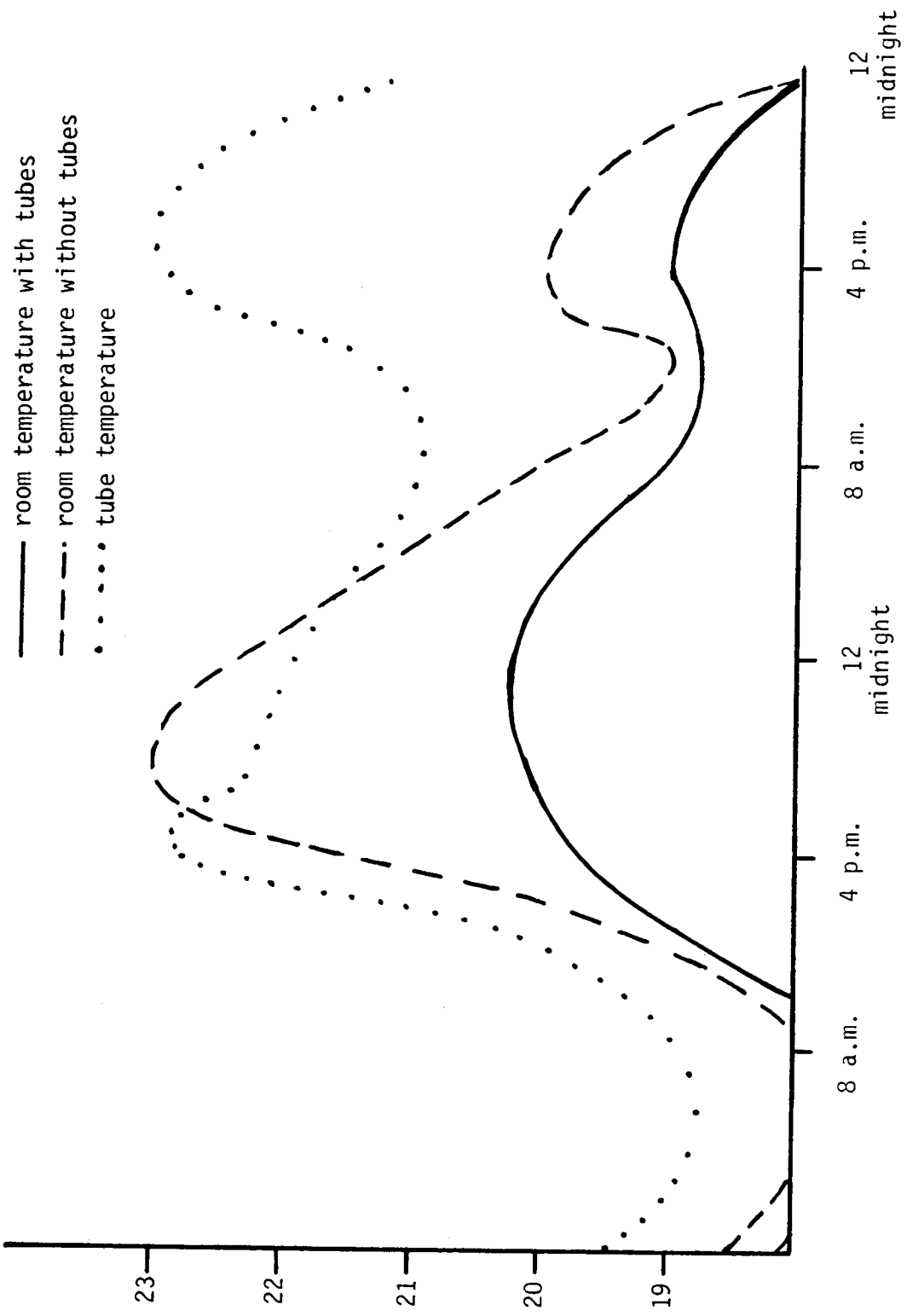


Figure 20. Room temperature with and without tubes

maintained a substantially lower room temperature than the version without tubes, while storing excess solar energy in the water. While the stored energy was not great enough to keep the room temperature above 18°C, the energy leaving the tubes was helping to make the back-up heat requirements of the version with tubes lower than the one without tubes.

As shown in Table 1, increasing the number of tubes from 20-24 lowered the auxiliary energy requirements a small amount. This increase in the number of tubes left less than 0.4 m^2 of glass without tubes behind it. Increasing the area of glass and number of tubes beyond the amounts in this version of the passive house would have required modification to the house layout and was not considered in this study.

An Evaluation of the MRT

Despite predictions by some authors that passive systems would have high MRT's, this was not the case with the passive modular house. The reason for the low MRT was threefold:

1. The tube temperatures rarely rose more than 2°C above room temperature.
2. The shape factor between a person in the center of the living room and the tubes was only 0.058.
3. The cold room surfaces, such as exterior walls and windows not covered by tubes, drew the MRT down.

Table 2 summarizes the effect of each room surface on the MRT during a six-hour period in January. An examination of this table reveals that it is unlikely that the MRT will be significantly above 18°C when the room temperature is at 18°C. This is the only situation where the MRT would cause a decrease in the back-up energy requirements.

TABLE 2

TEMPERATURE OF SURFACES USED TO CALCULATE THE MRT IN THE PASSIVE HOUSE
FROM 6:00 p.m. TO 12:00 MIDNIGHT ON JANUARY 3rd

	Temperatures (°C)									
Time	Ambient	Room	MRT	Tubes	South Glass Shades Down	East Window	East Wall	South Wall	Floor	Ceiling
6	10.00	18.13	18.37	22.31	17.20	14.90	17.77	18.07	17.94	18.02
7	8.90	18.12	18.31	22.07	17.08	14.46	17.69	17.87	17.89	17.98
8	8.30	18.10	18.25	21.84	16.99	14.20	17.59	17.71	17.86	17.92
9	8.30	18.06	18.19	21.62	16.95	14.18	17.51	17.61	17.70	17.86
10	6.70	18.01	18.09	21.41	16.72	13.51	17.41	17.52	17.68	17.79
11	6.10	18.00	18.05	21.20	16.65	13.27	17.36	17.47	17.67	17.76
12	5.60	18.00	18.03	21.01	16.66	13.07	17.31	17.42	17.66	17.75

Note: The temperature of the north wall, an interior wall, was assumed to be at a constant temperature of 18°C.

CHAPTER V

CONCLUSIONS

The Passive Modular House Computer Work

The computer program used in this study is a powerful tool for building simulation and design. The formulation of an experimentally verified tube model was a significant addition to the catalog of components in TRNSYS.

While model verification was limited due to time constraints, the extreme accuracy of the model during verification causes a great degree of confidence in the model's performance. Verification of the interaction between the tube and building is the only remaining task before the tube model can be considered to be completely supported by experimental results. This final verification needs a full winter of data to be done properly. Unfortunately, due to delays in house delivery, this work must be left to others.

The results of calculating the MRT of the living room of the passive house gave insight into the contribution of various surfaces in the room to the MRT. This study led to the conclusion that the impact of the MRT has been overstated in the literature. It is doubtful that the MRT will be significant in any passive design because of the low surface temperatures of the thermal storage systems unless the room has little or no glazing.

Additions made to the load calculator model during this study have greatly increased the model's flexibility. The impact of infiltration

on the heating load cannot be overemphasized. The variable infiltration method added in this work is vastly superior to the original method of selecting a constant number of air changes per hour. Finally, improvements to the window subroutine and the development of a radiation convertor during this study will provide increased accuracy and flexibility in future simulations.

The Passive Modular House Design

This study provided conclusive evidence that collecting solar energy with south-facing glass and using window insulation at night will significantly reduce the amounts of back-up energy required by a house for a heating season. This solar collector is efficient, simple, and inexpensive.

The contribution of the tubes in the passive modular house has also been quantified by this study. However, because their role has turned out to be less important than first thought, it is difficult to determine how necessary they are. The tubes represent a significant investment relative to the rest of the passive system and, in many houses, will increase the structural requirements. While it is not the purpose of this study to provide an economic analysis, it is obvious that a 10 percent decrease in the back-up energy needs of this small, well-insulated house does not represent a large savings. There are, however, certain intangible factors to be considered. The most important is that the mass storage reduces the temperature swings in the house, making it a more comfortable place in which to live. Secondly, the presence of the tubes reduced the glare that can be found in a direct gain system, without robbing the room of light like a masonry storage wall does.

It seems evident that as south glass-to-floor ratios rise above ten percent in a house of light-frame construction in this part of the country, addition of storage mass deserves strong consideration.

LIST OF REFERENCES

LIST OF REFERENCES

1. Holtz, M. et al. A Survey of Passive Solar Buildings, AIA Research Corporation for U.S. Department of Energy.

2. Mazria, Edward. The Passive Solar Energy Book, Rodale Press, Emmaus, Pennsylvania, 1979.

3. Fanger, P. O. Thermal Comfort Analysis and Applications in Environmental Engineering, McGraw-Hill, New York, New York, 1972, pp. 157-197.

4. Raber, B. F. and Hutchinson, F. W. Panel Heating and Cooling, John Wiley and Sons, Inc., New York, New York, 1947.

5. Baccei, B. "Mass Producing Low-Cost Passive Solar Buildings," Solar Age, December 1979, pp. 25-27.

6. Driggins, J. G., Project Engineer (TVA), Passive Solar Modular House, personal conversation, 1981.

7. Marshall Valuation Service, Marshall and Swift Publishing Company, Los Angeles, California, 1980.

8. "TVA--Designed Solar Homes to be for Sale Next Month," Knoxville News-Sentinel, Knoxville, Tennessee, August 27, 1980.

9. Sun-Lite High Performance Solar Collector Panels. Solar Components Division, Kalwall Corporation, Manchester, New Hampshire.

10. Sedrick, A. V. et al. "The Translucent Solar Storage Tube and its Application in Passive Heating Systems," Proceedings of the Fourth National Passive Solar Conference, Newark, New Jersey, 1979.

11. Clinton, J. R. et al. "Effects of Controls on Water Wall Performance," Procedures of the Second National Passive Solar Conference, Philadelphia, Pennsylvania, 1978.

12. Schnebly, J. et al. "The Window Quilt Insulating Shade," Procedures of the Second National Passive Solar Conference, Philadelphia, Pennsylvania, 1978.

13. Balcomb, J. D. et al. Passive Solar Work Shop, Knoxville, Tennessee, September 24-25, 1979.

14. Lumsdaine, M. Design Calculation Procedure for Passive Solar Houses, The University of Tennessee, 1979.

15. "Hand Calculator Programs for Passive Solar Design," Princeton Energy Group, Princeton, New Jersey.

16. Goldstein, D. B. et al. Design Calculations for Passive Solar Buildings by a Programmable Hand Calculator, University of California, Berkley, California, August 1979.

17. Analysis Methods for Solar Heating and Cooling Applications. The Solar Energy Research Institute, Golden, Colorado, January 1980.

18. Klein, S. A. et al. TRNSYS, A Transient Simulation Program, Solar Energy Laboratory, University of Wisconsin, Madison, Wisconsin, 1979.

19. Kusuda, T., Chairman of ASHRAE Subcommittee on Heating and Cooling Loads, in discussion following "Calculation of Transient Heat Flow Through Walls and Roof" by G. P. Mitalas, ASHRAE Transactions, Vol. 74, Part II, 1968.

20. ASHRAE Handbook of Fundamentals, American Society of Heating, Refrigeration, and Air Conditioning Engineers, New York, New York, 1977.

21. Stephenson, D. G. and Mitalas, G. P. "Cooling Load Calculations by Thermal Response Factors," ASHRAE Transactions, New York, New York, 1967.

22. DOE-2--Version 2.1. Prepared for the U.S. Department of Energy by Lawrence Berkley Laboratories and Los Alamos Scientific Laboratories, May 1980.

23. "Comparison Between Measured Computer-Predicted Hourly Heating and Cooling Energy Requirements for an Instrumented Wood Framed Townhouse Subjected to Laboratory Tests" (using NBSLD), ASHRAE Transactions, New York, New York, Vol. 81, Part III, 1975.

24. Mitalas, S. A. et al. "Transfer Function Method of Calculating Cooling Loads, Heat Extraction, and Space Temperature," ASHRAE Journal, ASHRAE, New York, New York, 1972.

25. Pawelski, M. J. Development of Transfer Function Load Models and Their Use in Modeling the CSU House I, A Thesis submitted for the degree of Master of Science, Mechanical Engineering, University of Wisconsin, Madison, Wisconsin, 1976.

26. Mitalas, G. P. and Arseneault, J. G. "Fortran IV Program to Calculate Z-Transfer Functions for the Calculation of Transient Heat Transfer Through Walls and Roof," 1970.

27. McAdams, W. H. Heat Transmission, McGraw-Hill, New York, New York, 1954.

28. Kimura, K. Algorithms for Building Heat Transfer Subroutines, ASHRAE, New York, New York, 1975.

29. Balcomb, J. D. et al. "Simulation Analysis of Passive Solar Heated Buildings--Comparison with Test Room Results," Proceedings of the 1977 Annual Meeting of the American Section of the International Solar Energy Society, Cape Canaveral, Florida, 1977.

30. Burns, P. J. et al. "Thermal Radiation Calculations for a Vertical Cylindrical Water Wall," Proceedings of the American Section of the International Solar Energy Society Fourth National Passive Conference, Vol. 4, 1979.

31. Threlkeld, J. L. Thermal Environmental Engineering, Prentice-Hall, Englewood Cliffs, New Jersey, 1970.

32. Dake, M. K. and Harleman, D. R. F. "Thermal Stratification in Lakes: Analytical and Laboratory Studies," Water Resources Research, April 1969.

33. Sissoms, L. E. and Pitts, D. R. Elements of Transport Phenomena, McGraw-Hill, New York, New York, 1972, pp. 249 and 605.

34. Tamura, G. T. "The Calculation of House Infiltration Rates," ASHRAE Transactions, Vol. 85, Part I, 1979.

35. Peterson, J. E. "Estimating Air Infiltration Rates into Houses: An Analytical Approach," ASHRAE Journal, New York, New York, January 1979.

36. Duffie, J. A. and Beckman, W. A. Solar Engineering of Thermal Processes, John Wiley and Sons, New York, New York, 1980.

37. Lui, B. Y. H. and Jordon, R. C. "The Interrelationship and Characteristic Distribution of Direct, Diffuse, and Total Solar Radiation," Solar Energy, Vol. 4, 1960, pp. 1-19.

38. Boes, E. C. et al. "Distribution of Direct and Total Solar Radiation Availabilities for the USA," Sharing the Sun, International Solar Energy Society, Vol. 1, 1976.

39. Lantz, L. J. and Winn, C. B. "Validation of Computer Models Used for Predicting Radiation Levels," Proceedings of the 1978 Annual Meeting of the American Section of the International Solar Energy Society, Vol. 2.2, 1978.

40. Hall, I. J. et al. "Generation of a Typical Meteorological Year," Proceedings of the 1978 Annual Meeting of the American Section of the International Solar Energy Society, Vol. 2.2, 1978.

41. Freeman, T. L. "Investigation of SOLMET Typical Meteorological Year," Proceedings of the 1979 Annual Meeting of the American Section of the International Solar Energy Society, 1979.

42. Hall, I. J. et al. "Solar Radiation Model Validation," Proceedings of the 1979 Annual Meeting of the American Section of the International Solar Energy Society, 1979.

APPENDICES

APPENDIX A

APPENDIX A

b AND d COEFFICIENTS FROM COMPUTER PROGRAM

(PASSIVE MODULAR HOME, TYPICAL WALL--TECH SITE)

Layer	Thickness	Conductivity	Density	Sp Heat	Resistance
1	0.0000	0.0000	0.0000	0.0000	0.3330
2	0.0365	0.1242	40.0000	0.2800	0.0000
3	0.0521	0.0208	6.5000	0.2300	0.0000
4	0.0104	0.0417	30.0000	0.3050	0.0000
5	0.2917	0.0322	6.5000	0.2195	0.0000
6	0.0208	0.0667	0.2900	0.3100	0.0000
7	0.0000	0.0000	0.0000	0.0000	0.6850

Thermal Conductance, U = 0.074 Sampling Time Interval, DT = 1.000

Coefficients for Ramp Input

J	D/B	1/B	A/B	D(Z)
0	0.566202	0.004934	0.203100	1.000000
1	-0.648113	0.031599	-0.178659	-0.377821
2	0.130865	0.010284	0.022808	0.009359
3	-0.001954	0.000183	-0.000249	-0.000010
4	0.000000	0.000000	0.000000	0.000000

APPENDIX B

APPENDIX B

ADDITION TO TRNSYS WINDOW MODEL VARIABLE

OUTSIDE CONVECTION COEFFICIENT

```
C** THIS STATEMENT DETERMINES WHICH SYSTEM OF UNITS WAS CHOSEN.
 100     IF (NU .EQ. 2.0) GO TO 450
         R = 0.04892*R
         HCRI = 20.4417468*HCRI
         TGABS = TGLAS+273.0
         TAABS = TE+273.0
         HRO = 0.20411E-6*((TGABS*TGABS+TAABS*TAABS)*(TGABS+
         !TAABS))*EMG

C** THIS STATEMENT DETERMINES WHICH RELATIONSHIP WAS CHOSEN
C
C** THIS IS KIMURA'S RELATIONSHIP FOR HCO USING SI UNITS
         RWD = WA+180.0-DIR
         IF (ABS(RWD) .GT. 180.0) RWD = 360.0-RWD
         IF (ABS(RWD) .GE. 90.0) GO TO 140
         IF (V .LE. 2.0) GO TO 150
         VC = 0.25*V
         GO TO 160
 150     VC = 0.5
         GO TO 160
 140     VC = .3+0.05*V
160      HCO = 3.28*((VC)**0.605)
         GO TO 130

C** THIS IS MCADAM'S RELATIONSHIP FOR HCO IN SI UNITS
 120     HCO = (5.7+(3.8*V))*3.6
         GO TO 170
 130     HCO = 20.4417468*HCO
 170     HCRO = HCO+HRO
         GO TO 500

C** THIS SECTION CALCULATES THE CONVECTION COEFFICIENTS IN
C** ENGLISH UNITS.
C
C** THIS IS KIMURA'S RELATIONSHIP FOR HCO USING ENGLISH UNITS
 450     V = 3.281*V
         IF (IHCO .EQ. 1) GO TO 220
         RWD = WA+180.0-DIR
         IF (ABS(RWD) .GT. 180.0) RWD = 360.0-RWD
         IF (ABS(RWD) .GE. 90.0) GO TO 240
         IF (V .LE. 2.0) GO TO 250
         VC = 0.25*V
         GO TO 260
  250    VC = 0.5
         GO TO 260
```

```
 240     VC = .3+0.05*V
 260     HCO = 3.28*((VC)**0.605)
         GO TO 230

C** THIS IS MCADAM'S RELATIONSHIP FOR HCO USING ENGLISH UNITS
 220     HCO = .99+(.21*V)
         TGABS = TGLAS+459.9
         TAABS = TE+459.9
         HRO = 0.1712E-8*((TGABS*TGABS+TAABS*TAABS)*(TGABS+
         1TGABS))*EMG
 230     HCRO = HCO+HRO

C** THE U VALUE OF THE GLASS OR GLASS AND NIGHT INSULATION
C** IS NOW CALCULATED.
 500     U = 1/((1/HCRO)+R+(1/HCRI))
         QT = AREA*U*(TE-TB)
```

APPENDIX C

APPENDIX C

KALWALL WATER TUBE MODEL

I. COMPUTER LISTING

```
      SUBROUTINE TYPE45 (TIME,XIN,OUT,T,DTDT,PAR,INFO)
C
C  THIS SUBROUTINE MODELS THE ENERGY BALANCE ON A KALWALL
C  TUBE. IN ADDITION, THIS MODEL PREDICTS THE MEAN RADIANT
C  TEMPERATURE IN A ROOM THAT THE TUBES ARE IN.
C
      DIMENSION XIN(15),OUT(30),T(1),DTDT(1),PAR(35)
      DIMENSION R(2),D(2),TAUP(2),RHOP(2),ALPHAP(2)
      DIMENSION RHO(182),ALPHA(182),CPH2O(2),CC3(2),CC4(2)
      DIMENSION SIGMA(2),CC1(2),CC2(2),GRAV(2),RHOREF(2)
      DIMENSION VISC(2),AB(2),HIUP(2),HIDN(2),HIHZ(2),V(2)
      DIMENSION UWIN(2),THETA(2),INFO(10),TAU(182),CC5(2)

      REAL NUSLT,NETSOL,MASS,MRT
      INTEGER D3,Z
      TAN(X) = SIN(X)/COS(X)

      DATA SIGMA/0.20411E-06,0.17141E-08/,CC1/0.0827,0.0133/
      DATA CC2/0.000232,0.0000021/,GRAV/9.8067,32.1742126/
      DATA RHOREF/353.0774,39.67545/,AB/273.2,459.76/
      DATA HIUP/33.318,1.63/,HIDN/22.0759,1.08/
      DATA PRNTL/0.72/,IUNIT/0/,PI/3.14159265/
      DATA ALPHA1/0.5006/,ALPHA2/1.1760/,ALPHA3/1.2868/
      DATA V/.0026598,.0087267/,VV/0.5/,CPH2O/4.174,1.00/
      DATA CC3/999.2,62.4/,CC4/0.194,0.0075/,CC5/10.0,50.0/
      DATA UWIN/11.86,0.58/,CC1/0.0827,0.0133/
      DATA DEGREE/57.29578/,HIHZ/29.843,1.46/

      IF (INFO(7) .GT. -1) GO TO 10
      IUNIT = INFO(1)
      INFO(5) = 1
      INFO(6) = 8
      INFO(9) =1
      CALL TYPECK(1,INFO,15,35,1)

C  SET PARAMETERS
      NU = INT(PAR(1)+0.1)
      HTL = PAR(2)
      RAD = PAR(3)
      NTUBES = PAR(4)
      REFFRP = PAR(5)
      XKLFRP = PAR(6)
      XKH2O = PAR(7)
      F12N = PAR(8)
      F12S = PAR(9)
```

```
      GAP = PAR(10)
      TAUGOG =PAR(11)
      FH2O = PAR(12)
      EMSFRP = PAR(13)
      EMSGLA = PAR(14)
      EMSWAL = PAR(15)
      ARADIG = PAR(16)
      ARADWL = PAR(17)
      FTUBES = PAR(18)
      FFLORS = PAR(19)
      FEWALS = PAR(20)
      FWWALS = PAR(21)
      FGLASS = PAR(22)
      FSWALS = PAR(23)
      FNWALS = PAR(24)
      FCEILS = PAR(25)
      ARFLOR = PAR(26)
      AREWAL = PAR(27)
      ARWWAL = PAR(28)
      ARSWAL = PAR(29)
      ARCEIL = PAR(30)
      ATGLAS = PAR(31)
      IWALL = PAR(32)
      AWIN = PAR(33)
      FWINS = PAR(34)
      GNOTUB = PAR(35)

C  THIS LOOP CALCULATES THE AVERAGE CHORD LENGTH IN THE
C  CIRCULAR CROSS SECTION OF A KALWALL TUBE.
C  THE CIRCLE IS MODLED BY HAVING A 360 SIDED POLYGON
C  INSCRIBED INSIDE IT.
      W = V(NU)
      WW = 0.5
      D17 = 0.0
      XX = 179.0
      DO 5 N = 1,360
      D16 = V(NU)*V(NU)+W*W-(2.0*V(NU)*W*COSD(179.0-WW))
      X = SQRT(D16)
      XSUM = X+D17
      XX = 179.0-WW
      WW = 180.0-XX-VV
      D17 = XSUM
      W = X
    5 CONTINUE
      AVCORD = XSUM/360.0
   10 CONTINUE

C  THE FOLLOWING EQUATIONS ARE A PORTION OF THE RADIATION
C  BALANCE ON THE TUBE.
      ARADI = PI*RAD*HTL
      DENOMS = ((1.0-EMSFRP)/EMSFRP*ARADI)+1.0/F12S*ARADI+
      1(1.0-EMSGLA)/(EMSGLA*ARADIG)
```

```
      DENOMN = ((1.0-EMSFRP)/EMSFRP*ARADI)+1.0/F12N*ARADI+
     1(1.0-EMSWAL)/(EMSWAL*ARADWL)

      IF(INFO(7) .GT. 0.0) GO TO 15

C  COLLECT INPUTS
      HB = XIN(1)
      HT = XIN(2)
      ZENAGL = XIN(3)
      AZMUTH = XIN(4)
      TA= XIN(5)
      TAUGLA = XIN(6)

      HD = HT-HB

      ANGLCD = AVCORD/COS(AZMUTH)

   15 CONTINUE
      TGLAS = XIN(7)
      TR = XIN(8)
      QEWALL = XIN(9)
      QWWALL = XIN(10)
      QCRAWL = XIN(11)
      QCEIL = XIN(12)
      QSWALL = XIN(13)
      DELTAT = XIN(14)
      RVALUE = XIN(15)

C  CALCULATE THE NATURAL CONVECTION COEFFICIENT FOR THE
C  SOUTH SIDE OF THE  WALL.
      TTUBE = T(1)
      TDIFF = ABS(T(1)-TR)
      TFS = (T(1)+TR)/2.0
      T1ABS = T(1)+AB(NU)
      TRABS = TR+AB(NU)
      TGABS = TGLAS+AB(NU)

C  CHECK TO SEE IF CONVECTION OCCURS
      IF(ABS(T(1)-TR) .LE. .001) GO TO 35

      AIRK = CC1(NU)+(CC2(NU)*TFS)
      RHO1 = RHOREF(NU)/T1ABS
      RHO2 = RHOREF(NU)/TRABS
      BETA = RHO2*((1.0/RHO1)-(1.0-RHO2))/(T(1)-TR)
      VISC(1) = (1.25E-04)+(5.46E-07*TFS)
      VISC(2) = (1.28E-05)+(1.06E-07*TFS)
      GRSHOF = (GRAV(NU)*BETA*(T(1)-TR)*(HTL**3.0))/
     1(VISC(NU)**2.0)
      PRGRSH = GRSHOF*PRNTL
      IF (PRGRSH .GT. 10E9) GO TO 20
      NUSLT = .59*(PRGRSH**.25)
      GO TO 30
```

```
 20      NUSLT = .13*(PRGRSH**.3333333)
 30      HTC1 = NUSLT*AIRK/HTL
         GO TO 38
 35      HTC1 = 0.0

C  CHECK TO SEE IF IT IS DAYLIGHT
 38      IF (HT .LT. 0.000001) GO TO 300

C  CHECK TO SEE IF THE SHADES ARE CLOSED
         IF (RVALUE .GT. 0.1) GO TO 300

C  CALCULATION OF SOLAR INCIDENCE ANGLE WHERE SUNAGL IS
C  GREATER THAN 0 OR LESS THAN ALPHA1.
         ABSAZ = ABS(AZMUTH)
         D1 = 90.0-ABSAZ
         IF (AZMUTH .GT. 0.0) GO TO 40
         TUBAGL = D1-10.0
         GO TO 50
 40      TUBAGL = D1+10.0

C CHECK TO SEE IF BEAM RADIATION HITS THE TUBES
 50      IF (TUBAGL .LE. 0.0) GO TO 140
         IF (HB  LE. 0.0) GO TO 140
         SUNAGL = TUBAGL/DEGREE
         IF (SUNAGL .GT. ALPHA1) GO TO 60
         ARC = 1.5708-ALPHA1+SUNAGL
         IF (AZMUTH) 100,110,110
 60      IF (SUNAGL .GT. ALPHA2) GO TO 70
         X2 = RAD/SIN(SUNAGL)
         B = 2.0*RAD+GAP X2
         RR = PI-SUNAGL
         A = B*COS(RR)+SQRT(B*B*COS(RR)*COS(RR)+RAD*RAD-B*B)
         ARG = ((B*B+RAD*RAD-A*A)/(RAD*2.0*B))
         AA = ACOS(ARG)
         DD = SUNAGL-AA
         ARC = 1.5708+DD
         IF (AZMUTH) 100,110,110
 70      IF (AZMUTH .GT. ALPHA3) GO TO 80
         X2 = RAD/SIN(SUNAGL)
         E = 2.0*RAD+GAP-X2
         F = E*COS(SUNAGL)-SQRT(E*E*COS(SUNAGL)*COS(SUNAGL)
         1-RAD*RAD+E*E)
         ARG2 = ((E*E+RAD*RAD-F*F)/(2.0*RAD*E))
         FF = ACOS(ARG2)
         ARC = 1.5708+SUNAGL+FF
         IF (AZMUTH) 100,110,110
 80      ARC = 3.1416
         IF (AZMUTH) 100,110,110

C  COMPUTE VALUES OF AZIMUTH OF THE FLATS WHICH COMPRISE THE
C  SURFACE OF THE TUBE.
 100     VARIAZ = AZMUTH+90.0-ARC*DEGREE
```

```
      GO TO 120
110   VARIAZ = AZMUTH-90.0
120   D25 = ARC*DEGREE
      D3 = IFIX(D25)
      VARIAZ = VARIAZ+0.5
      DO 130 I = 2,D3+1
      D4 = AZMUTH-VARIAZ
      ALTAGL = 90.0-ZENAGL
      D5 = COSD(D4)*COSD(ALTAGL)
      D7 = ACOS(D5)
      THETA(I) = D7
      VARIAZ = VARIAZ+1.0
130   CONTINUE
140   THETA(1) = 60.0/DEGREE

C  THIS LOOP CALCULATES TAU TUBE, RHO TUBE, ALPHA TUBE, AND
C  THEN SUMS THE THE SOLAR ENERGY IN EACH CATEGORY.
      DO 150 K = 1,D3+1
      THETA1 = THETA(K)
      THETA2 = ASIN(SIN(THETA1)/REFFRP)
      R(1) = (SIN(THETA2-THETA1)*SIN(THETA2-THETA1))/
     1(SIN(THETA2+THETA1)*SIN(THETA2+THETA1))
      R(2) = (TAN(THETA2-THETA1)*TAN(THETA2-THETA1))/
     1(TAN(THETA2+THETA1)*TAN(THETA2+THETA1))
      TAB=EXP(-XKLFRP/COS(THETA2))
      DO 170 L= 1,2
      TAUP(L) = TAB*((1.0-R(L))/(1.0+R(L)))*(1.0-(R(L)*
     1R(L)))/(1.0-(R(L)*TAB*R(L)*TAB))
      RHOP(L) = R(L)*(1.0+TAB*TAUP(L))
      ALPHAP(L) = (1.0-TAB)*(1.0-R(L))/(1.0-(R(L)*TAB))
170   CONTINUE
      TAU(K) = (TAUP(1)+TAUP(2))/2.0
      RHO(K) = (RHOP(1)+RHOP(2))/2.0
      ALPHA(K) = (ALPHAP(1)+ALPHAP(2))/2.0
      IF (HB .LE. 0.0) GO TO 160
      IF (TUBAGL .LE. 0.0) GO TO 160
150   CONTINUE

C  CALCULATE BEAM AND DIFFUSE RADIATION PASSING THROUGH THE
C  GLASS.
      GO TO 200
160   HB = 0.0
      ARC = 0.0
200   TBGLAS = TAUGLA*HB
      TDGLAS = TAU60G*HD

C  CALCULATE THE DIFFUSE RADIATION TRANSMITTED AND ABSORBED BY
C  THE TUBE WALL.
      GLSTUB = ATGLAS-GNOTUB
      TDTTOT = TDGLAS*TAU(1)*GLSTUB/NTUBES
      ADTTOT = TDGLAS*ALPHA(1)*GLSTUB/NTUBES
      RDTTOT = TDGLAS*RHO(1)*GLSTUB/NTUBES
```

```
      D14 = 0.0
      D15 = 0.0
      D20 = 0.0

C  SUM THE BEAM RADIATION THAT IS TRANSMITTED OR ABSORBED BY
C  THE TUBE WALL.
      DO 190 M = 2,D3+1
      TBTUBE = TBGLAS*TAU(M)*COS(THETA(M))*(1.0/DEGREE)*
     1RAD*HTL
      ABTUBE = TBGLAS*ALPHA(M)*COS(THETA(M))*(1.0/DEGREE)*
     1RAD*HTL
      RBTUBE = TBGLAS*RHO(M)*COS(THETA(M))*(1.0/DEGREE)*
     1RAD*HTL
      TBTTOT = TBTUBE+D14
      ABTTOT = ABTTOT+D15
      RBTTOT = RBTTOT+D20
      D14 = TBTTOT
      D15 = ABTTOT
      D20 = RBTTOT
  190 CONTINUE

C  CALCULATE THE AMOUNT OF SOLAR ENERGY PASSING THROUGH THE
C  WATER IN THE TUBE AND OUT THE NORTH WALL AND THE AMOUNT
C  OF SOLAR ENERGY REFLECTED OFF OF THE TUBES, ABSORBED
C  BY THE TUBES, OR MISSING THE TUBES.
      QTTUBE = (TBTTOT+TDTTOT)
      QTHRU = QTTUBE*(1.0-FH20)*EXP(-XKH20*ANGLCD)*TAU(1)
      ATUBE = PI*2.0*RAD*HTL
      ATUBES = ATUBE*NTUBES
      DNOTUB = GNOTUB*TDGLAS
      QRTUBS = (RDTTOT+RBTTOT)*NTUBES
      QATUBS = (ADTTOT+ABTTOT)*NTUBES
      QTTUBS = QTTUBE*NTUBES
      TBTUBS = (TBTTOT+RBTTOT+ABTTOT)*NTUBES
      TBTGLA = TBGLAS*ATGLAS
      BNOTUB = TBTGLA-TBTUBS
      QNOTUB = DNOTUB+BNOTUB

      GO TO 310
  300 QTTUBE = 0.0
      QTHRU = 0.0
      ADTTOT = 0.0
      ABTTOT = 0.0
      TBGLAS = 0.0
      TDGLAS = 0.0
      RBTTOT = 0.0
      RDTTOT = 0.0
      QNOTUB = 0.0
      ARC = 0.0
      QRTUBS = 0.0
      QATUBS = 0.0
      QTTUBS = 0.0
```

```
      BNOTUB = 0.0
      DNOTUB = 0.0

C  CALCULATE THE MASS OF ONE TUBE AND THE SURFACE AREA OF
C  ALL OF THE TUBES.
  310 DENH2O = CC3(NU)-CC4(NU)*(T(1)-CC5(NU))
      MASS = PI*RAD*RAD*HTL*DENH2O
      ATUBE = PI*2.0*RAD*HTL
      ATUBES = ATUBE*NTUBES

C  CALCULATE THE RADIATION COEFFICIENTS FOR THE NORTH AND
C  THE SOUTH SIDE OF THE WATER WALL FROM PREVIOUS
C  HOUR'S DATA.
      HTC2 = SIGMA(NU)*(TGABS*TGABS+T1ABS*T1ABS)*
     1(T1ABS+TGABS)
      HTC3 = SIGMA(NU)*(TRABS*TRABS+T1ABS*T1ABS)*
     1(T1ABS+TRABS)

C ENERGY BALANCE ON A KALWALL TUBE WITH TUBES ON EITHER
C  SIDE OF IT.
      NETSOL = ADTTOT+ABTTOT+QTTUBE-QTHRU
      RADSTH = (HTC2*ARADI*(T(1)-TGLAS))/DENOMS
      RADNTH = (HTC3*ARADI*(T(1)-TR))/DENOMN
      TOTRAD = -RADSTH-RADNTH
      CONV = -(HTC1*ATUBE*(T(1)-TR))
      DTDT(1) = (NETSOL+TOTRAD+CONV)/(MASS*CPH2O(NU))

C  CALCULATE THE MEAN RADIANT TEMPERATURE OF THE ROOM.
      QWINDC = AWIN*UWIN(NU)*(-DELTAT)
      TFLOOR = TR+(QCRAWL/(HIDN(NU)*ARFLOR))
      TWIN = TR+(QWINDC/(HIHZ(NU)*AWIN))
      IF (QCEIL .GT. 0.0) GO TO 500
      HI = HIUP(NU)
      GO TO 600
  500 HI = HIDN(NU)
  600 TCEIL = TR+(QCEIL/(HI*ARCEIL))
      IF (IWALL) 700,800,900
  700 TEWALL = TR
      TWWALL = TR
      GO TO 1000
  800 TEWALL = TR
      QNET = QWWALL-QWINDC
      TWWALL = TR+(QNET/(HIHZ(NU)*ARWWAL))
      GO TO  1000
  900 TWWALL = TR
      QNET = QEWALL-QWINDC
      TEWALL = TR+(QNET/(HIHZ(NU)*AREWAL))
 1000 TNWALL = TR
      TSWALL = TR+(QSWALL/(HIHZ(NU)*ARSWAL))
      MRT = (FCEILS*TCEIL)+(FEWALS*TEWALL)+(FWWALS*TWWALL)
     1+(FSWALS*TSWALL)+(FGLASS*TGLAS)+(FFLORS*TFLOOR)
```

```
     1+(FNWALS*TNWALL)+(FTUBES*T(1))+(FWINS*TWIN)

C  CALCULATE AND LABEL THE OUTPUTS
      TTUNEW = T(1)
      ESTORD = MASS*CPH2O(NU)*TTUNEW*NTUBES
      OUT(1) = -CONV*NTUBES
      OUT(2) = RADSTH*NTUBES
      OUT(3) = RADNTH*NTUBES
      OUT(4) = ESTORD
      OUT(5) = MRT
      OUT(6) = QNOTUB
      OUT(7) = QTHRU*NTUBES
      OUT(8) = TTUNEW
      OUT(9) = ARC*DEGREE
      OUT(10) = BNOTUB
      OUT(11) = HTC1
      OUT(12) = TBGLAS
      OUT(13) = TDGLAS
      OUT(14) = HTC3
      OUT(15) = HTC2
      OUT(16) = (RADNTH+RADSTH)*NTUBES
      OUT(17) = QRTUBS
      OUT(18) = (TBGLAS+TDGLAS)*ATGLAS
      OUT(19) = QTTUBS
      OUT(20) = QATUBS
1500  CONTINUE
      RETURN
      END
```

II. IDENTIFICATION OF VARIABLE NAMES FOR TUBE MODEL

Variname	Description
IUNIT	Unit number (read off of model)
INFO	TRNSYS control array (see manual)
NU(1)	I = SI units 2 = Eng. units
HTL	Height of water tube
RAD	Tube radius
REFFRP	Refractive index for fiberglass (FRP)
XKLFRP	Extinction coefficient for fiberglass
XKLH2O	Extinction coefficient for water
F12N	Shape factor, one tube to north wall
F12S	Shape factor, one tube to south window
GAP	Gap between tubes
TAU6OG	Transmittance at 60 of glass from type 35
FH2O	Amount of sunlight absorbed at surface of water
EMSFRP	Emittance of Kalwall tube (FRP)
EMSWAL	Emittance of south glass of north wall
ARADIG	Area of glass receiving radiation from one tube
ARNWAL	Area of north wall receiving radiation from one tube
FTUBES	Shape factor tubes to subject
X	An unknown cord length in the circle
XSUM	Sum of all cord lengths in the circle
AVCORD	Average cord length

Variname	Description
ANGLCD	Average distance traveled through water
HB	Beam radiation on the glass type 16
HD	Diffuse radiation on the glass type 16
ZENAGL	Solar zenith angle (degrees) type 16
AZMUTH	Solar azmuth angle (degrees) type 16
TA	Ambient temperature reader
TAUGLA	Transmittance glass type 35
TGLAS	Temperature south glass type 42
TR	Temperature room type 19
QEWALL	Heat transfer east wall type 17
QWWALL	Heat transfer east wall type 17
QCRAWL	Heat transfer crawl space type 19
QSWALL	Heat transfer south wall type 17
DELTAT	Temperature difference room and ambient
RVALUE	R value of night insulation
TFS	Film temperature of room
T1ABS	Absolute temperature of room
TRABS	Absolute temperature of room
TGABS	Absolute temperature of south glass
FFLORS	Shape factor floor to subject
FEWALS	Shape factor east wall to subject
FWWALS	Shape factor west wall to subject
FGLASS	Shape factor south glass to subject
FSWALLS	Shape factor south wall to subject
FCEILS	Shape factor ceiling to subject

Variname	Description
ARFLOR	Area floor in MRT room
AREWAL	Area east wall in MRT room
ARWWAL	Area west wall in MRT room
ARSWAL	Area south wall in MRT room
ARCEIL	Area ceiling in MRT room
ATGLASS	Total area of glass south side
IWALL	-1 both east and west walls interior 0 east wall interior, west wall exterior 1 west wall interior, east wall exterior
AWIN	Area of non-south window
FWINS	Shape factor non-south window and subject
GNOTUB	Area of south glass with no tubes behind it
W	Side of triangle in polygon in one-inch-diameter circle for computing average cord length (see sketch)
WW	Angle opposite side W
D17	Dummy variable
XX	Angle in triangle mentioned under W
D16	Dummy variable
AIRK	Thermal conductivity of air
BETA	Coefficient of volumetric expansion evaluated at T film
VISC	Viscosity of air at T film
PRGRSH	Prandtl-Grashof number
NUSLT	Nusselt number
HTC1	Convection coefficient for tubes
VARIAZ	Variable azmuth of flats on the tube

Variname	Description
SUNAGL	-Angle between projection of sun's azmuth on horizontal to line perpendicular to 10 west of south (i.e., south wall of house) in degrees
ARC	Curve of tube hit by beam radiation
THEATA(1)	60 (theta is in radians)
ALTAGL	Altitude angle
THETA1	Angle of incidence
THETA2	Angle of refraction
R(1)	Perpendicular component of light p 171 Duffie and Beckman
TAB	Transmittance with absorptance neglected
TAUP1	Transmittance of perpendicular component
TAUP2	Transmittance of parallel component
RHOP1	Reflectance perpendicular component
RHOP2	Reflectance parallel component
ALPHAP(1)	Absorptance perpendicular component
QTHRU	Total beam and diffuse through tube
ATUBE	Area of one tube
ATUBES	Area of all tubes
DNOTUB	Diffuse radiation missing tube
QRTUBS	Total radiation reflected off of all tubes
QATUBS	Total radiation absorbed by all tubes
QTTUBS	Total radiation transmitted by all tubes
TBTUBS	Total beam radiation striking all tubes
TBTGLA	Total beam radiation entering the south glass
BNOTUBS	Beam radiation missing tubes
QNOTUB	Total radiation entering glass and not striking a tube

Variname	Description
DENH2O	Density of water
CC3	Density of water at 50°F
CC4,CC5	Straight line density change per °F 50°F to 90°F
HTC2	Radiation calculation north side of tube to the room
HTC3	Radiation calculation south side of tube to glass
ARADI	180-degree area of tube radiating north or south
DENOMS	Two-body enclosure (see Sissom and Pitts, p. 250)
DENOMN	S = south N = north
ALPHAP(2)	Absorptance parallel component
TAU(k)	Transmittance tube wall at k angle of incidence
RHO(k)	Reflectance tube wall at k angle of incidence
ALPHA(k)	Absorptance tube wall at k angle of incidence
TBGLAS	Beam transmitted by glass per meter^2
GLSTUB	Amount of glass with tubes behind it
TDGLAS	Diffuse transmitted by south glass per meter^2
TDTTOT	Total diffuse transmitted through south side of one tube
ADTTOT	Total diffuse absorbed through south side of one tube
RDTTOT	Total diffuse reflected off of south side of one tube
TBTUBE	Beam transmitted through south side of tube L high by (r) x (l) wide
ABTUBE	Absorbed beam radiation south side of tube L high by (r) x (l) wide
RBTUBE	Reflected beam radiation through south side of tube L high by (r) x (l) wide
TBTTOT	Total beam transmitted through south arc of tube

Variname	Description
ABTTOT	Total beam absorbed by south arc of tube
RBTTOT	Total beam reflected by south arc of tube
QTTUBE	Total beam and diffuse transmitted by south arc of tube
DTDT(1)	Temperature H_2O in the tube
TFLOOR	Temperature floor
HIDN	Down heat flow free convection from ASHRAE
UWIN	U value non-south glass double-pane window
QWINDC	Conduction through non-south glass window
TWIN	Temperature window in east wall assuming no absorptance of radiation
HIHZ	Horizontal heat flow free convection from ASHRAE
TCEIL	Temperature ceiling
TEWAL	Temperature east wall
TWWAL	Temperature west wall
TNWAL	Temperature north wall
MRT	Mean radiant temperature at center of room

Outputs

(1)	Convective loss off of all tubes
(2)	Radiation loss off of south side of all tubes
(3)	Radiation loss off of north side of all tubes
(4)	Energy stored in all tubes
(5)	Mean radiant temperature
(6)	Total radiation entering south glass not caught by the tubes
(7)	Energy transmitted through all tubes

(8)	Temperature of the tube
(9)	Amount of tube hit by beam radiation (in degrees)
(10)	New tube temperature
(11)	Convection coefficient of tube
(12)	Total beam radiation through the glass
(13)	Total diffuse radiation through the glass
(14)	Radiation coefficient north side of tube
(15)	Radiation coefficient south side of tube
(16)	Total radiation off of tubes
(17)	Radiation reflected off of all tubes
(18)	Total radiation transmitted through the glass
(19)	Total radiation transmitted by all of the tubes
(20)	Total radiation absorbed by all of the tubes

APPENDIX D

APPENDIX D

CALCULATION OF EXTINCTION COEFFICIENT OF KALWALL SUNLITE MATERIAL

This development uses equations given in Duffie and Beckman.[36] Kalwall gave the transmittance (at zero angle of incidence) to be 0.883 and the index of refraction to be 1.58 for their Sunlite panels.[9]

A combination of Fresnel's laws at zero angle of incidence, when one medium is air, gives an equation for reflectance of:

$$\rho_r = \frac{I_r}{I_i} = \left(\frac{n - 1}{n + 1}\right)^2 \tag{28}$$

where subscript r denotes that absorptance has not been accounted for. Solving for ρ_r, we get 0.050538.

At zero angle of incidence, the perpendicular and parallel components of ρ_r are equal; therefore:

$$\rho_r/2 = \rho_{||r} = \rho_{\perp r} = 0.02527 \tag{29}$$

Duffie and Beckman give an equation for the total transmittance, τ, as a function of τ_a and τ_r:

$$\tau = \frac{\tau_a}{2}\left(\frac{1 - \rho_{||r}}{1 + \rho_{||r}}\right)\left(\frac{1 - (\rho_{||r})^2}{1 - (\rho_{||r} \cdot \tau_a)^2}\right) + \left(\frac{1 - \rho_{\perp r}}{1 + \rho_{\perp r}}\right)\left(\frac{1 - (\rho_{\perp r})^2}{1 - (\rho_{\perp r} \cdot \tau_a)^2}\right) \tag{30}$$

This equation is the average of the parallel and perpendicular components reflectance and accounts for both reflectance and absorptance. Solving Equation (30) for τ_a gives a value of 0.929.

Bourger's law relates τ_a and the extinction coefficient in the following manner:

$$\tau_a = e^{-KL} \tag{31}$$

L is known; its value is 0.001016 meters. Solving Equation (31) for K gives a value of 72.6 m^{-1} for the extinction coefficient.

APPENDIX E

APPENDIX E

SHAPE FACTOR CALCULATION--SOUTH WALL

The following shape factor calculations between an individual in the center of the living room of the passive modular house (sitting at any orientation) and the components of the south wall of that room were prepared using charts developed by Fanger.[3]

(all dimensions in meters)

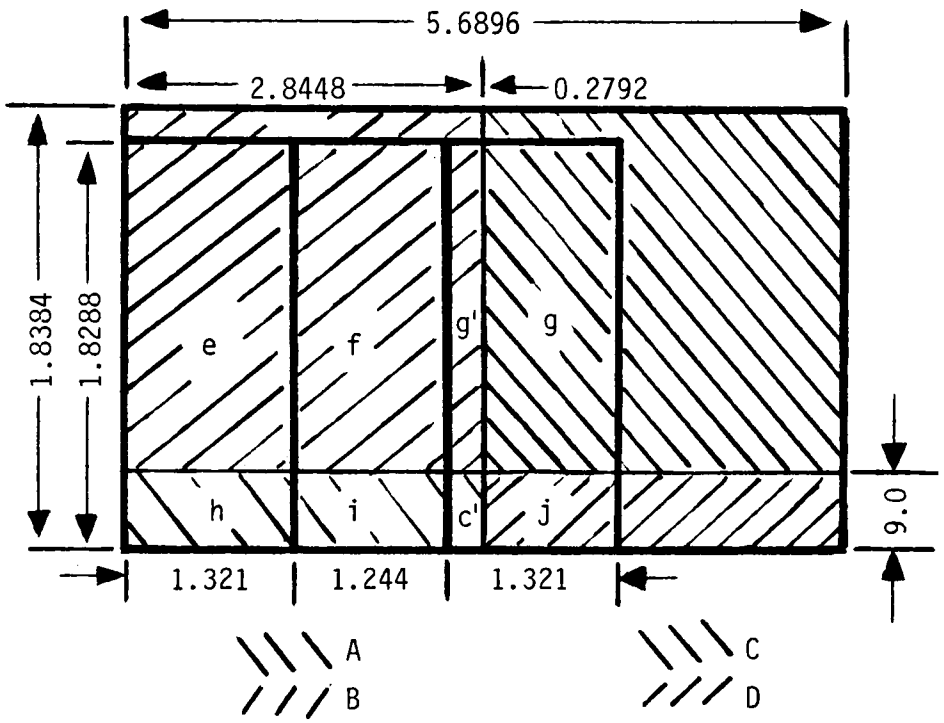


Figure 21. South wall of living room in passive modular house

$F_{p-A} = F_{p-D} = 0.056$	$\frac{b}{c} = 1.06$	$\frac{a}{c} = 1.65$
$F_{p-B} = F_{p-C} = 0.025$	$\frac{b}{c} = 0.35$	$\frac{a}{c} = 1.65$
$F_{p-g} = 0.023$	$\frac{b}{c} = 0.711$	$\frac{a}{c} = 0.551$
$F_{p-j} = 0.009$	$\frac{b}{c} = 0.317$	$\frac{a}{c} = 0.551$
$F_{p-fg'} = 0.034$	$\frac{b}{c} = 0.711$	$\frac{a}{c} = 0.882$
$F_{p-ic'} = 0.020$	$\frac{b}{c} = 0.347$	$\frac{a}{c} = 0.882$
$F_{p-g'} = 0.002$	$\frac{b}{c} = 0.711$	$\frac{a}{c} = 0.1616$
$F_{p-c'} = 0.001$	$\frac{b}{c} = 0.347$	$\frac{a}{c} = 0.1616$
$F_{p-efg'} = 0.045$	$\frac{b}{c} = 0.711$	$\frac{a}{c} = 1.647$
$F_{p-hic'} = 0.035$	$\frac{b}{c} = 0.347$	$\frac{a}{c} = 1.647$

tubes e + h:

$$F_{p-efg'} - F_{p-fg'} = 0.011$$
$$+ F_{p-c'ih} - F_{p-c'} = 0.015$$
$$= 0.026$$

tubes g + j:

$$F_{p-g} + F_{p-g'} = 0.025$$
$$+ F_{p-j} + F_{p-c'} = 0.010$$
$$= 0.035$$

$$F_{p-tubes} = 0.061$$

$$\text{Window} = F_{p-fg'} - F_{p-g'} = 0.032$$

$$F_{p-window} = 0.032$$

$$F_{p-south\ wall} = F_{p-ABCD} = 0.167$$
$$- F_{p-tubes} = -0.061$$
$$- F_{p-wall} = -0.026$$
$$= 0.067$$

VITA

Thomas W. Allen was born May 22, 1953, in Okaloosa County, Florida. He graduated from Donelson High School in Nashville, Tennessee in 1971. In 1975, he received his Bachelor of Science Degree in Mechanical Engineering from Tennessee Technological University in Cookeville, Tennessee.

Following four and one-half years as a Mechanical Engineer with the Aluminum Company of America in Alcoa, Tennessee, Mr. Allen resigned to attend graduate school full-time. He received his Professional Engineers License in 1980 and graduated from The University of Tennessee, Knoxville with a Master of Science Degree in Mechanical Engineering in August of 1981.

Mr. Allen will marry Miss Nancy A. Sentell in October of 1981. They will reside in Nashville, Tennessee, where Mr. Allen will join the mechanical engineering firm of Smith, Seckman, and Reid, Incorporated.